STUDIES OF ORBITAL ELECTRON CAPTURE BY SCINTILLATION COUNTER METHODS.

BY

B.R. JOSHI.

PRESENTED TO THE UNIVERSITY OF GLASGOW

AS A THESIS FOR THE DEGREE OF Ph.D.

JULY, 1961.

ProQuest LLC.
789 East Eisenhower Parkway
P.O. Box 1346
Ann Arbor, MI 48106 – 1346

PREFACE.

Considerable theoretical interest lies in the measurements of the L/K capture and K/β^+ branching ratios, but in most cases, particularly for the middle and high atomic number elements, the experimental accuracies are far from being satisfactory enough to be compared profitably with the relevant theory. This arises from the technical difficulties associated in the detection and analysis of the soft X-rays and Auger electrons which accompany capture transitions.

Chapter I contains a brief account of the general theory of β-decay and a discussion of the theory of L/K capture, and K/β^+ branching ratio. The interpretation of the Fierz interference term, in the light of recent development of β-decay theory, which can be derived from the K/β^+ measurements, is presented. The results of the theory which have a direct bearing on the present work and a review of the more reliable experimental results on the subjects are also given.

A description of the new well-type technique developed for the measurement of the L/K capture ratios for the middle and high atomic number elements is given in

Chapter II. This technique eliminates the need for the surface escape corrections.

The next three chapters respectively deal with the experimental measurements on the L/K capture ratios for the allowed transitions Cs^{131} and Ba^{131}, and for the "unique" first forbidden transition Tl^{204}. The determination of the Fierz interference term from the K/β^+ ratio in pure Gamow-Teller interaction of Co^{58} is presented in Chapter VI. The β^- spectral branch in Tl^{204} has also been reinvestigated and the results extended down to 10 KeV. There were no previous measurements on the L/K ratios for Cs^{131}, Ba^{131} and Tl^{204} and the present experimental results provide a critical examination of the validity of the theory. The measurement on Co^{58} is of sufficient accuracy to enable a closer limit to be put on the Fierz interference term. Suggestions regarding the future applications of the technique particularly for the study of higher order processes in the electron capture transitions are presented in chapter VII.

The author shares a joint responsibility with Dr. G.M. Lewis for the development of the technique and the work on Cs^{131} and Co^{58}. The rest is entirely his own.

I would like to thank Professor P.I. Dee for his interest and encouragement throughout the course of this research. To Dr. G.M. Lewis I would like to express my sense of gratitude and thanks for the supervision of this work and for his valuable discussions. I would also like to thank Mr J.T.Lloyd and the staff of the stores and the workshop for their prompt technical assistance.

I am grateful to the Colombo Plan Authorities for a Research Fellowship and to the Government of Nepal for its sponsorship and for the leave of absence.

July, 1961. B.R. Joshi.

CONTENTS

PUBLICATIONS.

On the Measurement of Orbital Electron Capture with particular reference to ^{131}Cs.

B.R. Joshi and G.M. Lewis, Proc. Phys. Soc., 76, 349, (1960).

Orbital Electron Capture Ratio and Beta Spectrum of ^{204}Tl.

B.R. Joshi, Proc. Phys. Soc., 77, 1205, (1961).

Determination of the Fierz Interference Term from the K-Capture/β^+ Ratio for the Pure Gamow-Teller Decay of Co^{58}.

B.R. Joshi and G.M. Lewis, accepted for publication in the Proc. Phys. Soc.

CHAPTER I

GENERAL INTRODUCTION

The main features of the beta-decay can be described as nuclear transitions between states of equal mass number resulting in the creation and/or destruction of light particles called leptons ($\beta^{\pm}$ and neutrino). It is necessary for single beta-decay that the nuclear charge should change by unity. The principle of the conservation of angular momentum together with the conservation of statistics, and the number of heavy particles as experimentally observed imply that the beta-decay must involve the direct interaction of four particles called fermions (spin $\frac{1}{2}$). These four particles are two nucleons, a neutron (n) and a proton (p) and two leptons, an electron (e^- or e^+) and a neutrino (ν or $\bar{\nu}$). The beta-decay process can be represented by

$n \rightarrow p + e^- + \bar{\nu}$	negatron-emission
$p \rightarrow n + e^+ + \nu$	positron-emission
$p + e^- \rightarrow n + \nu$	electron-capture
$(n + e^+ \rightarrow p + \bar{\nu})$	positron-capture

The last, included for symmetry, is associated with the hypothetical positron capture.

Positron emission can also be regarded as the

inverse of negatron emission, an electron and an anti-neutrino being drawn from the negative energy sea and being absorbed in the nucleus:

$$p + e^- + \bar{\nu} \rightarrow n,$$

the 'hole' left by the absorption of electron and anti-neutrino appearing as the anti-particles, a positron and a neutrino.

The first successful theoretical formulation of beta decay was developed by Fermi in 1934. The theory was based on the neutrino hypotheses put forward by Pauli (1933), to enable the maintenance of the conservation of energy and spin in beta decay. The neutrino was assigned a vanishing small rest mass with neutral charge and $\frac{1}{2}$ spin. According to Fermi, beta decay is generated in proportion to the four-vector current density associated with the intertransformation of a charged and a neutral particle (neutron $\leftrightarrow$ proton, electron $\leftrightarrow$ neutrino). The mathematical structure was similar to one which was used to describe the electromagnetic interactions of photons with charged particles. It predicts the shape of the beta spectrum and the relationship between the half life and transition energy.

This information was useful for the knowledge of spin and parity change involved in the transitions and was used as an additional data in constructing the decay scheme.

By the end of 1956 the nature of weak interactions which underlie beta-decay seemed to be becoming clearer. The five interaction coupling constants appearing in the interaction Hamiltonian and represented by scalar (C_S), vector (C_V), tensor (C_T), axial vector (C_A) and pseudoscalar (C_P) were reduced to C_S and C_T together with a small proportion of C_P term (Jackson 1958). The remaining question was the relative magnitude and sign of these terms. Then followed a revolution in the understanding of beta-decay. This started with the well known $\tau - \theta$ puzzle which led Lee and Yang (1956) to examine the question of parity conservation in weak interactions. They pointed out that the existing experimental evidence was mainly based on the measurements of scalar quantities such as allowed, forbidden and unique forbidden beta spectral shapes, beta-neutrino correlation and beta-gamma correlation. None of these experiments would answer the parity question as these

will not measure the interference terms between the coupling constants for the parity conserving and parity non-conserving terms. One must measure a pseudoscalar formed out of the experimentally measured quantities. Lee and Yang suggested several experiments that would test the validity of parity conservation in weak interactions. The first experimental demonstration of parity non-conservation was carried out by Wu et al (1957) on the decay of $Co^{60} \rightarrow Ni^{60} + e^{-} +$ (neutrino). They observed a large asymmetry in the intensity of beta-particles from polarised Co^{60} nuclei with the preference of emission antiparallel to the direction of nuclear spin. This experiment further showed that charge conjugation is also not conserved. No experiments exist regarding the time reversal invariance. Since then several experiments have been done in the field of beta-decay (Konopinski 1959) as well as in mu- and pi-meson decays (Jackson 1958) which have all confirmed the non-conservation of parity in weak interaction. This followed in the introduction of parity non-conserving coupling constants C'_S, C'_V, C'_T, C'_A

and C'_P in addition to the previous parity-conserving constants C_S, C_V, C_T, C_A and C_P. Moreover, recent experimental evidence is in favour of C_V and C_A interaction instead of the former C_S and C_T. This is discussed in page 22 in connection with Fierz interference term.

Following the discovery of parity non-conservation in weak interactions Lee and Yang (1957) as well as Salam (1957) and Landau (1957) have proposed a two-component theory of the neutrino. In such a theory the spin of neutrinos must be completely polarised parallel or anti-parallel to their direction of motion. In case of positron emission, the associated neutrinos have left-handed spin (i.e. anticlockwise as seen from the nucleus), and the antineutrinos, which accompany negatrons, have right-handed. In order to satisfy the relativistic invariance the mass of the neutrino should be identically zero.

The two-component neutrino theory combined with the principle of lepton conservation accounts for the observed non-conservation of parity and charge conjugation in weak interactions.

In recent years there has been considerable increase in experimental data in the field of beta-decay by beta-emission and this has greatly helped the understanding of beta interaction. The subject has been reviewed by Konopinski (1959). However, comparatively very little experimental work has been done in the electron capture process. This arises from the technical difficulties encountered in the efficient detection and analysis of the soft x-rays or Auger electrons associated with the electron capture transitions. Therefore the work on electron capture was undertaken here with a new internal source scintillation counter technique developed by the author. But, before giving a detailed description of this technique (in Chapter II) it is necessary to give a brief review of the theory of orbital electron capture which has a direct bearing on the experimental work presented in this thesis.

ORBITAL ELECTRON CAPTURE

The main interest in the study of orbital electron capture transitions are twofold. In the first place the capture of an electron from the electron cloud of an

atom by the proton of the nucleus indicates the influence of the atomic electrons on nuclear properties. Secondly, electron capture is essentially a proton-neutron transition in the nucleus arising from the coupling between the nucleons and leptons. In this respect the electron capture studies give information, as in case of beta-decay by beta-emission, of the associated weak-interactions responsible for the transition.

The experimental parameters of interest in electron capture transitions, which serve as a basis for useful comparison with relevant theory, are the relative probabilities of L- and K-capture events, or the K-capture/ positron branching ratios, which are of main concern in this thesis, and the higher order processes such as inner bremsstrahlung energy distribution and 'shake off' electron distribution following capture events.

Yakawa and Sakata predicted theoretically electron capture in 1935. Two years later Alvarez (1937) demonstrated K-capture for V^{48} by using a thin walled Geiger Muller counter. Since then more than 150 isotopes have been identified to decay by electron

capture, mostly by capturing electrons from the K-shell of the atom. L-shell capture, which occurs with a lesser probability than that of a K-electron, was shown experimentally by Pontecorvo et al for A^{37} in 1949.

In electron capture the energy released in the transition is not detected. It is postulated that the neutrino carries off the available energy if there is no gamma emission. In general an electron capture transition can be represented by

$$(p) + e^{-} \rightarrow (n) + \nu \qquad (1)$$

Here the bracket indicates that the proton and the neutron are bound to the other nucleons in the nucleus, and ν referes to the neutrino emitted following capture. If the masses of the initial and final atoms are M_1 and M_2 respectively electron capture can occur energetically when the following relation is satisfied

$$M_1 - M_2 > |E_n| \qquad (2)$$

Here $|E_n|$ is the binding energy of the electron in the n^{th} state. The corresponding energy released from capture is given by

$$q_n \simeq \Delta M + \Delta\epsilon - |E_n| \qquad (3)$$

representing $\Delta M = M_1 - M_2$ and $\Delta\epsilon$ the reduction in

energy corresponding to the change in atomic binding energy. $\Delta\epsilon$ is generally negligible. The recoil energy of the final nucleus is very small and is neglected. The rest mass of the neutrino is very small or identically zero in the light of two-component theory and can be considered as wholly kinetic (in analogy with photon except the difference in spin).

For positron emission the energy condition which must be fulfilled is

$$M_1 - M_2 \geq 2m_o c^2 + \epsilon_v \qquad (4)$$

Here ϵ_v is the binding energy of the valency electron in the parent atom and is generally very small. Positron emission is always accompanied by electron capture, and occurs mainly from the K-shell. Even when the transition energy is sufficient for positron emission, it often happens that orbital electron capture is predominant.

In certain cases the capture from the K-shell is energetically forbidden. In such cases capture from L and higher shells could still occur.

ELECTRON CAPTURE TRANSITION PROBABILITIES

The transition probabilities for K-capture was calculated by Yakawa and Sakata (1935), Bethe and Bacher (1936) and Møller (1937) on the same lines as the theory of beta-decay by beta-emission by Fermi (1934). The expression involves the wave functions of the electron and the neutrino evaluated at the nucleus and the nuclear matrix element. The equations developed for beta-emission in general (Konopinski 1953) may be applied to electron capture with minor changes: (a) the electron wave functions are those of the bound electrons instead of free electrons and, (b) the electron energy being discrete, the neutrino energy is also discrete. In general, transition probabilities depend not only on the properties of the nucleus, but also on the characteristics of the captured electron, which are influenced by the size of the nucleus, and the properties of the electron cloud surrounding the nucleus. Moreover, electron capture, like beta-emission, also depends on the energy, spin and parity associated with the initial and final nuclear states.

The allowed transitions, which occur with the

largest probability, correspond to the selection rule: $\Delta I = 0$ or 1 and no. Recent evidence (see p. 22) indicates that the beta decay interaction is a mixture of V (vector) and A (axial-vector). The transitions with $\Delta I = 0$ are produced by either V or by A. But the $0 \rightarrow 0$ transitions are produced only by the V and are called Fermi. The transitions with $\Delta I = 1$ are produced only by the A and are called Gamow-Teller.

For allowed transitions the K-capture decay constant is given by the expression

$$\lambda_K = \frac{g^2}{4\pi^2} |M|^2 q_K^2 g_K^2 (1 + b) \qquad (5)$$

where g is the universal beta-decay constant,

$$|M|^2 = (C_V^2 + C_V'^2)|M_F|^2 + (C_A^2 + C_A'^2)|M_{GT}|^2$$

neglecting C_S and C_T terms,

q_K is the energy given to the neutrino in K-capture ($q_K = E - \epsilon_K$, E is the electron capture transition energy and ϵ_K the K-shell binding energy),

g_K is the radial part of the "large" component of the Dirac wave function of the K-electron evaluated at the nucleus,

and b is the Fierz interference term.

The nuclear matrix element M consists of Fermi M_F and Gamow-Teller M_{GT} parts. As a good approximation the value of g_K^2 is given by the following expression:

$$g_K^2 = \frac{1 + \gamma}{2\Gamma(2\gamma + 1)} R^{2\gamma - 2} (2\alpha Z')^{2\gamma + 1} \qquad (6)$$

where $\gamma = 1 - \epsilon_K$, $Z' = Z - \sigma$, σ being the screening correction factor and is approximately equal to 0.3, $R = 3.9 \times 10^{-13} \times A^{1/3}$, the nuclear radius in units of $\hbar/mc$

and $\alpha = \frac{1}{137}$ is the fine structure constant.

In allowed transitions, the capture takes place mainly from the L_I subshell and with a small proportion from L_{II} subshell. The L_{II} contribution never exceeds more than ten percent of the L_I and falls off rapidly for low atomic number elements. Capture from the L_{III} subshell is generally negligible. The L_{II} subshell differs from L_I in parity but has the same angular momentum. The L_{III} subshell has a different angular momentum and hence it has a different selection rule.

For allowed transitions.the decay constant for the L-capture probabilities is given by

$$L_I + L_{II} = \frac{g^2}{4\pi^2} |M|^2 \, q_L^2 \, (g_{L_1}^2 + f_{L_{II}}^2)(1 + \beta) \qquad (8)$$

where g_{L_I} and $f_{L_{II}}$ are the "large" and "small" components of the Dirac wave functions for the L_I and L_{II} electrons.

q_L is the energy given to the neutrino in L-capture ($q_L = E - \epsilon_L$, ϵ_L is the L shell binding energy).

The difference in binding energy between L_I and L_{II} subshells can practically always be neglected.

The transitions with $\Delta I = 2$, $\Delta\pi = -1$ are first forbidden "unique" transitions. They are characterised by a unique matrix element. The K, $L_I + L_{II}$ and L_{III} orbital capture transition probabilities are given by the general relations:

$$K = \frac{g^2}{36\pi^2} |M'|^2 \, q_K^4 \, g_K^2 \, (1 + b) \tag{9}$$

$$L_{I+II} = \frac{g^2}{36\pi^2} |M'|^2 \, q_L^4 (g_{L_I}^2 + f_{L_{II}}^2)(1 + b) \tag{10}$$

and

$$L_{III} = \frac{g^2}{4\pi^2} |M'|^2 \, q_L^2 R^{-2} g_{L_{III}}^2 \, (1 + b) \tag{11}$$

where $|M'|^2 = (|C_A|^2 + |C_A'|^2)|M_{GT}|^2$;

and R is the nuclear radius.

The angular momentum for L_{III} electron is one unit

greater than that of L_I or L_{II}. This introduces an additional factor $(qR)^{-2}$ which enhances the L_{III} contribution.

L/K CAPTURE RATIO

Allowed Transitions ($\Delta I = 0$ or 1, no)

The L/K capture ratio for allowed transitions can be obtained from the equations (5) and (8) of the preceeding section. The capture ratio is given by

$$\frac{\lambda_L}{\lambda_K} = \left(\frac{q_L}{q_K}\right)^2 \left(\frac{g_{L_I}^2 + f_{L_{II}}^2}{g_K^2}\right) \qquad (12)$$

Marshak (1942) used Dirac radial wave functions with Slater screening to compute $\frac{g_{L_I}^2 + f_{L_{II}}^2}{g_K^2}$. Rose and Jackson (1949) used Hartree self-consistent field wave functions for low atomic number elements and relativistic wave functions for a Thomas-Fermi atom for other values. They constructed a graph of $\frac{g_{L_I}^2}{g_K^2}$ as a function of Z.

More recently Brysk and Rose (1955 and 1958) have carried out extensive numerical calculations on the

Dirac radial wave functions of K, L_I, L_{II} and L_{III} electrons, using machine computation. They have taken into account the corrections arising due to the secondary effects of the finite nuclear size, variation of the electron wave functions over the nuclear volume, and the screening. The results have been extended to include forbidden transitions.

The Dirac radial wave functions consist of "large" and "small" components. The "large" components make a contribution in the allowed and the "unique" forbidden transitions and are denoted by g_K, g_{L_I}, $f_{L_{II}}$ and $g_{L_{III}}$, the "small" components are f_K, f_{L_I}, $g_{L_{II}}$ and $f_{L_{III}}$. In general f^2 is small and g^2 can be expected to vary as $\frac{1}{n^3}$ where n is the principal quantum number. So as a first order approximation equ.(12) becomes

$$\frac{\lambda_L}{\lambda_K} = \left(\frac{q_L}{q_K}\right)^2 \frac{1}{8} \qquad (13)$$

In the approximation of large radial distance the L_{II} contribution is given by

$$\frac{f^2_{L_{II}}}{g^2_{L_I}} = \frac{3}{16} \alpha^2 Z^2 \qquad (14)$$

This ratio varies between $2\frac{1}{2}\%$ to 8% for Z between 50 to 80 and falls off rapidly with decreasing Z.

If the electron capture transition energy is much higher than the K- or L-shell binding energy so that $q_K \simeq q_L$, eq. (12) reduces to

$$\frac{\lambda_L}{\lambda_K} = \frac{g_{L_I}^2 + f_{L_{II}}^2}{g_K^2} \qquad (15)$$

<u>First Forbidden "Unique" Transition</u> ($\Delta I = 2$, yes)

From equs. (9), (10) and (11), the capture ratio would be

$$\frac{\lambda_{L_I} + \lambda_{L_{II}}}{\lambda_K} = \left(\frac{q_L}{q_K}\right)^4 \left(\frac{g_{L_I}^2 + f_{L_{II}}^2}{g_K^2}\right) \qquad (16)$$

$$\frac{\lambda_{L_{III}}}{\lambda_K} = \frac{9q_L^2}{q_K^2 R^2} \quad \frac{g_{L_{III}}^2}{g_K^2} \qquad (17)$$

The equ. (16) shows that the L_{III}-capture is favoured with low transition energy for "unique" transitions. Even for high transition energy the magnitude of L_{III} contribution is comparable with L_{II}

and for the energy corresponding to the positron threshold ($2\ moc^2 \simeq 1$ MeV) L_{III}/L_{II} ratio is of the order of unity. It shows little Z-dependence and varies from 1 for Z = 15 to 0.2 for Z = 95.

For allowed and "unique" forbidden transitions, the L/K-capture ratios are independent of the nuclear matrix element as in these cases a single element occurs in the numerator and denominator which cancel out automatically. This is not the case in the forbidden transitions in which the multiplicity of matrix elements hampers precise comparison between the theoretical and the experimental capture ratios. The knowledge of matrix elements is very poor. So measurements on the L/K-capture ratios for the allowed and "unique" forbidden transitions only can provide critical check of the relevant theory.

Further amendment to the theory of orbital electron capture ratio has been made by Odiot and Daudel (1956) ~~1958~~). They have treated the electron wave functions taking into account the correlations which exist among the positions of the atomic electrons. This was shown to increase the theoretical L/K value by a factor

of 10 for He (Z = 2), 2 for Be (Z = 3) and by about 25% for Ar (Z = 18). However, the correction falls off rapidly as Z increases and becomes insignificant for middle and high Z elements.

K-CAPTURE TO POSITRON RATIO AND THE FIERZ INTERFERENCE TERM.

For allowed transitions, the probability per unit time that a positron is emitted with energy between W and W + dW is given by Fermi's formula

$$N(W)dW = \frac{g^2}{2\pi^3}|M|^2 F(Z,W)pW(W_o-W)^2dW(1-\frac{\gamma b}{W}) \qquad (18)$$

in which $\gamma = (1 - \alpha^2Z^2)^{\frac{1}{2}}$, $\alpha = \frac{1}{137}$ and M is the nuclear matrix element given by

$$|M|^2 = (|C_S|^2 + |C_S'|^2 + |C_V|^2 + |C_V'|^2)|M_F|^2 +$$

$$(|C_T|^2 + |C_T'|^2 + |C_A|^2 + |C_A'|^2)|M_{GT}|^2$$

here M_F and M_{GT} are the Fermi and Gamow-Teller matrix element respectively, C_X referes to the well known coupling constants for the X-th interactions (i.e. S, V, T, A, or P, the pseudoscalar P being absent for allowed decays), and the dashes the parity non-conserving

terms, F(Z,W) is Fermi's function for allowed decays, p is the positron momentum, W_o the total energy (including the rest mass) available for the transition and, Z the nuclear charge which is negative for positron emitters.

The total transition probability is obtained by integrating eq. (18) which is

$$\lambda_+ = \frac{g^2}{2\pi^3} |M|^2 \int_1^{W_o} F(Z,W)\ pW(W_o - W)^2\ dW\left(1 - \frac{\gamma b}{W}\right) \qquad (19)$$

The F function which takes into consideration the correction due to Coulomb field acting on the positrons is given by Feister (1952) in zero order approximation and by Dzelepov and Zirianova (1952) with second order correction. These must be corrected to allow for the effect of nuclear radius and of screening. The former, which is about 1%, has been evaluated by Rose and Holmes (1951) and the latter by Reitz (1950). The screening effect becomes important for Z greater than 16 (See Perlman et al 1958).

The term b is the Fierz interference term (1937) and arises due to the interference between the scalar (S) and vector (V) interactions in Fermi and the tensor

(T) and axial-vector (A) in Gamow-Teller transitions respectively. b is given by the general expression

$$b=2Re\frac{(C_S C_V^* + C'_S C'^*_V)|M_F|^2 + (C_T C_A^* + C'_T C'^*_A)|M_{GT}|^2}{(|C_S|^2 + |C_V|^2 + |C'_S|^2 + |C'_V|^2)|M_F|^2 + (|C_A|^2 + |C_T|^2 + |C'_A|^2 + |C'_T|^2)|M_{GT}|^2} \quad (20)$$

here the star (*) denotes complex conjugate.

From equs. (5) and (19) the K/β^+ ratio for allowed transitions is given by

$$\frac{\lambda_K}{\lambda_+} = \frac{\pi/2\; q_K^2\; g_K^2(1+b)}{\int_1^{W_o} F(Z,W)\; pW(W_o - W)^2\; dW(1 - \frac{\gamma b}{W})} \quad (21)$$

For b = 0, the eq.(2) becomes

$$\left(\frac{\lambda_K}{\lambda_+}\right)_{b=o} = \frac{\pi/2\; q_K^2\; g_K^2}{\int_1^{W_o} F(Z,W)\; pW(W_o - W)^2\; dW} \quad (22)$$

From equs. (21) and (22) then

$$\frac{\lambda_K}{\lambda_+} = \frac{1+b}{1 - b\gamma\langle W^{-1}\rangle}\left(\frac{\lambda_K}{\lambda_+}\right)_{b=o} \quad (23)$$

$$\text{here } \langle W^{-1}\rangle = \frac{\int_1^{W_o} F(Z,W)\; pW(W_o - W)^2\; \frac{1}{W}\; dW}{\int_1^{W_o} F(Z,W)\; pW(W_o - W)^2\; dW} \quad (24)$$

The quantity $\langle W^{-1} \rangle$ can be obtained by averaging W^{-1} over the theoretical positron spectrum by graphical integration method.

The theoretical value of K-capture/β^+ branching ratios have been calculated by Zweifel (1957), Perlman et al (1958) and more recently by Nguyen-Khac (See Depommier et al 1960). Nguyen-Khac has used Dzelepov and Zirianova's tables with second order corrections (1952) for β^+ emission and Brysk and Rose's curves (1955, 1958) for the radial functions of the bound K-shell electron. He has also taken into account nuclear radius (finite size) and screening effects. Experimental results have been reviewed by Perlman et al (1958), Konijn et al (1958) and Bouchez and Depommier (1960). Distinction should be made between the total electron capture/β^+ ratio and K-capture/β^+ ratio while refering to the above review articles.

For allowed and "unique" forbidden transitions, the nuclear matrix elements cancel out the numerator and denominator of the K-capture/β^+ branching ratio. So the Fierz interference term b can be determined by inserting the experimental and the theoretical values for

K-capture/β^+ ratios given by $\frac{\lambda_K}{\lambda_+}$ and $\left(\frac{\lambda_K}{\lambda_+}\right)_{b=o}$ respectively in eq(23).

The interpretation of the Fierz interference term has changed in recent years, following the introduction of the two-component neutrino theory and the increase in beta-decay data. Before the overthrow of parity conservation in weak interaction, a small value of b implied that either C_A/C_T or C_T/C_A in Gamow-Teller and C_V/C_S or C_S/C_V in Fermi interactions were small. The two-component theory requires a combination of the coupling constants in the form $C_X = \pm C'_X$ where X = S,V,T,A or P. For allowed transitions P would be absent. If the interaction is invariant under time reversal the coupling constants will be real. For Gamow-Teller decay the experiment of Herrmannsfeldt et al (1958) on the recoil energy spectrum from He^6 showed that $(|C_A|^2 + |C'_A|^2)$ is large compared to $(|C_T|^2 + |C'_T|^2)$. For Fermi transitions the recoil experiment for both Ne^{19} and A^{35} by Herrmannsfeldt et al (1957, 1958) showed that $(|C_V|^2 + |C'_V|^2)$ is greater than $(|C_S|^2 + |C'_S|^2)$. The longitudinal polarisation experiments on the Gamow-Teller

β^- radiation of Co^{60} by Frauenfelder et al (1957) and the Fermi radiation of both Ga^{66} and Cl^{34} by Deutsch et al (1957) and Boehm et al (1957) showed that the relation $C_A = +C_A'$ and $C_V = +C_V'$ holds. These results are supported by the Goldhaber, Grodzins and Sunyar experiment (1958) on Eu^{152}. They studied the resonant scattering of gamma-rays with a Sm_2O_2 scatterer and observed those events in which the gamma-ray and neutrino go in opposite direction. From this they found that the neutrinos emitted are left-handed. Both $C_T = +C_T'$, $C_T = -C_T'$ and $C_S = +C_S'$, $C_S = -C_S'$ are consistent with two-component theory. Hence the present evidence demands the following choice of coupling constants

$$\begin{aligned} & C_A = +C_A' , \quad C_T = -C_T' \\ \text{or} \quad & C_A = +C_A' , \quad C_T = +C_T' \end{aligned} \tag{25}$$

and

$$\begin{aligned} & C_V = +C_V' , \quad C_S = -C_S' \\ \text{or} \quad & C_V = +C_V' , \quad C_S = +C_S' \end{aligned} \tag{26}$$

In the form $C_A = +C_A'$, $C_T = -C_T'$ and $C_V = +C_V'$, $C_S = -C_S'$

eq. (20) shows that b should vanish identically. On the other hand, if $C_A = +C_A'$, $C_T = +C_T'$ and $C_V = +C_V'$, $C_S = +C_S'$; b does not vanish.

Restricting attention to pure Gamow-Teller transitions, which is the main concern in this thesis, the experimental values of b are necessary to check the validity of the two-component neutrino theory if $C_T = -C_T'$ or to delimit further the maximum magnitude of C_T and C_T', if $C_T = +C_T'$. Moreover, the expression for the electron polarisation experiments, designed to examine the validity of the theory and the relative magnitudes of C_T, C_T', contains b explicitly. The polarisation P is given by

$$P = \frac{Ap/W}{1+b/W}$$

here
$$A = \pm \frac{2\mathrm{Re}(C_T C_T'^{*} - C_A C_A'^{*})}{(|C_T|^2 + |C_T'|^2 + |C_A|^2 + |C_A'|^2)} \qquad (27)$$

From this point of view also it is desirable to know the magnitude of b experimentally.

Apart from the assessment of the Fierz interference term, the measurement of K-capture/β^+ ratio provides several important pieces of information. For allowed and "unique" forbidden decay the nuclear matrix element cancels out

the denominator and the numerator of the theoretical expression of the K-capture/β^+ ratio. So the measure of the K-capture/β^+ branching ratio provides a good comparison of the validity of beta-decay theory. In addition, it provides information concerning the magnitude of the finite nuclear size and second order corrections on the transition probabilities. As belief on the theory of branching ratio grows stronger, a precise measurement of the K-capture/β^+ ratio could be most useful in determining the energy available for the transition. This, in principle, can be done by comparing the calculated and measured branching ratios. Since branching ratios are sensitive to the transition energy, this application can be very useful or even better than the value obtained from beta-spectrum studies.

As this chapter is mainly devoted to the theoretical description of the subject it may be convenient to include here the theory of "unique" beta-spectrum referred to in Chapter V in connection with the work on Tl^{204}.

THE "UNIQUE" FORBIDDEN BETA SPECTRUM

The "unique" forbidden transitions provide one of the strong pieces of evidence for the existence of Gamow-Teller interactions because they could arise only from A or T coupling. They are characterised with spin change $\Delta I = n + 1$ and parity change $\Delta\pi = (-1)^n$ where $n = 1,2$ and 3. One of the most significant features of the "unique" spectra is that the Fermi-Kurie plot shows a distinct "S" shape (Langer et al 1949). This could be linearised with proper shape correction factor. The energy distribution for β^- emission is given by

$$N(W)dW = \frac{g^2}{2\pi^3} |M'|^2 F(+Z,W)\, pW(W_o - W)^2 dW\left(1+\frac{\gamma b}{W}\right) a_n \qquad (28)$$

here $|M'|^2 = (|C_T|^2 + |C'_T|^2 + |C_A|^2 + |C'_A|^2)\, M_{GT}^2$

and a_n is the shape correction factor. The expressions for a_n, taking into account the coulomb effect on the electron, is given by Konopinski (Siegbahn p.305, 1955) as

$$a_n = \sum_{\nu=o}^{n} \frac{(2n+1)!\,(2\nu+1)!}{2^{2\nu}(\nu!)^2(2n-2\nu+1)!}\, q^{2(n-\nu)}\, L_\nu(p,+Z) \qquad (29)$$

here $q = (W_o - W)$, L_ν is the tabulated function of Rose Perry and Dismuke (Siegbahn App.II) For the first forbidden "unique" transitions (n = 1), the expression (29)

gives the shape factor:

$$a_1 = q^2 Lo(p_1, + Z) + 9qL_1(p_1, + Z) \qquad (30)$$

In general the shape factor a_n is insensitive to the Coulomb effect for "unique" transitions. This is not the case with most types of forbidden spectra. However, for high atomic number elements, as in the case of Tl^{204} (Z = 81), the simplified formula based on low Z approximation (Siegbahn p.304) was found to be inadequate by Wu (Siegbahn p. 331) to give a linear Fermi-Kurie plot.

From eq. (28) with b = 0 n = 1 and $G = (\frac{p}{W})F$, it follows that

$$\left[N(W)/Ga_1\right]^{\frac{1}{2}}/W = K(W_o - W) \qquad (31)$$

here $K = (\frac{g^2}{2\pi^3} |M'|^2)^{\frac{1}{2}}$ and is independent of W. The values of G are given by Rose, Perry and Dismuke (Siegbahn App. II) and Z refers to the daughter nucleus. The left hand side of this equation plotted against W is known as a corrected Fermi-Kurie plot. Such a plot will yield a straight line, the intercept of which with the W axis giving the transition energy. Without the shape correction factor (a = 1), this will show a

distinct "S" shape for "unique" spectra.

EXPERIMENTAL DATA OF L/K-CAPTURE RATIOS

There are three principal methods which have been used to measure L/K capture ratios: external source, coincidence technique and internal source spectroscopy.

External Source Spectroscopy

The radioactive source is kept outside the sensitive volume of a detector which is in general a thin window proportional or a scintillation counter and the relative intensities of K and L x-rays are measured. Large corrections for the source scattering, self absorption and variation of detection efficiency with energy must be applied. Some of the L- and K-shell vacancies are filled by Auger transitions. So a knowledge of K- and L-fluorescence yield of the daughter element are required. These are not accurately known. This introduces considerable uncertainty in the results. For Ge^{71} the experimental value of Langevin (1954,1955) of 0.30 becomes about 0.15 when the measured value of 0.53 of Drever et al (1956) is used instead 0.45 given

by Burhop (1952). Moreover, the x-ray intensity ratio must be allowed for the fraction of K_α x-rays which could spuriously record as L-capture event. In view of this the external source method is considered to be inadequate for a reliable check of the relevant theory.

Coincidence Technique

This technique is similar to the indirect technique used for the measurement of the K-capture/β^+ ratio as described below. In this case it is necessary that the capture should proceed to an excited state of the daughter element followed by a high energy gamma-ray transition. This method also involves inaccuracies in the data regarding fluorescence yield, the relative intensity of K_α x-rays, and the gamma-ray detection efficiency.

Internal Source Spectroscopy.

The radioactive source is thoroughly dispersed in the sensitive volume of the detector. The source thickness would be negligibly small so there would be no

source self-absorption or scattering. In the proportional counter application the source is introduced in the counter in a suitable gaseous form. The advantage of the method is that the knowledge of K and L fluorescence yield is not required. If the counter is large enough and the pressure of the filling gas is high (6 atmos for Z = 35) essentially all the L-capture events which consist of L x-rays or L-Auger-electrons would be completely absorbed for elements with atomic number of the order of 35 or less. The K-capture events would comprise of K x-rays or K-Auger-electrons. K-Auger would be completely absorbed in the filling gas. But some of the K_α x-rays could escape undetected from the counter and would record as a spurious L-capture event. To overcome this Drever et al (1956) developed an ingenious proportional counter technique. They used two concentric proportional counter system without the intervening wall. The escaping K_α x-rays from the main central counter were detected in the outer ring counter which was used as an anticoincidence pulse. Thus the false recording of L-events arising due to the escape of K_α x-rays could be avoided. The loss of K-

events was compensated by choosing a suitable design so that the same number of K x-rays entered the ring counter from the insensitive space at the ends. This method gives L/K-capture ratio directly from the observed L-and K-peaks.

An internal source scintillation counter method has been used by der Mateosian (1953). Scintillation crystal of NaI(Tl) was grown with a trace of the source being studied. The L/K-capture ratio was deduced from the K x-ray peak and the intensity of the low energy gamma-ray, assuming each gamma-ray accompanies the capture transition. More recently, Scobie and Gabathuler (1958) produced an internal source of I^{126} by irradiation of a NaI(Tl) crystal in a gamma-ray beam of a Synchrotron by $I^{127}(\gamma,n)I^{126}$ reaction.

The L/K-capture ratio has been determined for a number of nuclei. The most comprehensive review of the experimental results up to 1960 has been given by Robinson and Fink (1960) and Bouchez and Depommier (1960). The majority of the cases are done by indirect technique and in many cases the electron capture decay energies are not known. So these results are not

suitable for comparison with the theory. However, there are a few cases, mainly at low Z elements ($Z \lesssim 40$), in which the electron capture transition energies are known and the L/K-capture ratios have been measured by internal source technique. These measurements which are precise enough to be compared with the theory of Brysk and Rose (1955, 1958) are made for the simple allowed decays of A^{37}, Fe^{55}, Co^{58}, Ge^{71}, Kr^{79} and for the parity forbidden decay of I^{126}. The results of these measurements as compared with the theoretical value with the name of the author and the date of the experiment are shown in figure 1. Figure 1 shows that the experimental results are 10 to 20% higher than the theoretical values. For A^{37} the theoretical value of L/K = 0.08 increases to 0.10 when the effect of correlations existing between the positions of the electrons proposed by Odiot and Daudel is taken into consideration.

EXPERIMENTAL DATA OF K-CAPTURE/β^+ RATIO AND THE FIERZ INTERFERENCE TERM.

Extensive reviews of the total electron capture/β^+

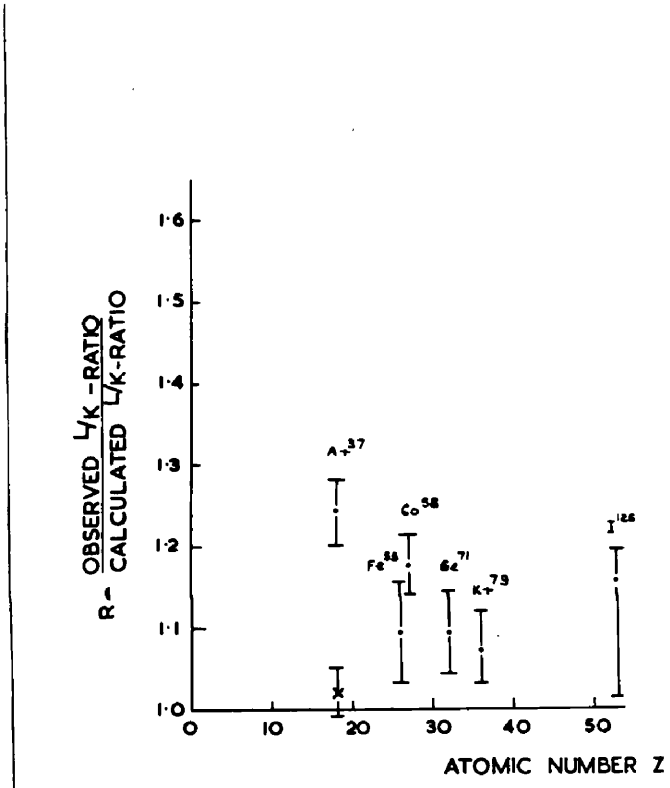

Fig. 1.

Comparison of the experimental and the calculated results of L/K capture ratios. The uncertainty in R is represented by the vertical bars. The cross for Ar^{37} denotes the value with the Odiot and Daudel correction. ($18Ar^{37}$ by Santos-Ocampo and Conway, 1960; $26Fe^{55}$ by Scobie, Moler and Fink, 1959; $27Co^{58}$ by Moler, 1961; $32Ge^{71}$ by Drever and Moljk, 1957 and communicated by Drever, 1959; $36Kr^{79}$ communicated by Drever, 1959; $53I^{126}$ by Scobie and Gabathuler, 1958).

ratio meausrements are given by Radvanyi (1955), Perlman et al (1958), Konijn et al (1958) and Bouchez and Depommier (1960). Mainly two methods have been used: direct and indirect. The direct method consists in a meausrement of the x-rays or Auger electrons following capture. The positron intensity is measured from the β^+ spectrum or the annihilation gamma-rays. In the indirect method it is necessary that the transition proceeds to an excited state of the daughter nucleus which subsequently emits a gamma-ray. Then the intensity measurement of the gamma-rays gives the total rate of decay by total electron capture and positron emission. The rate of decay by positron emission is generally measured by taking coincidences between the gamma-rays on the one side and the β^+-particles or the annihilation photons on the other.

Among the direct methods, the internal gaseous source proportional counter technique with the provision for the elimination of escape corrections, developed by Drever and Moljk (1957), gives results on K-capture/β^+ ratios with better accuracy. When a solid source is used and the K x-rays are measured in a counter it is

necessary to estimate the absolute counter efficiency and the correction required for the x-ray absorption in the source and counter window. This is not easy to ascertain with sufficient accuracy. On the other hand, if the Auger-electrons and the positrons are measured in the same counter, the need for determining counter efficiency can be avoided. However, in this case the self-absorption and scattering of Auger-electrons would be most severe. Similarly, indirect methods have, too, their own limitations. Considerable systematic errors may arise from the instrumental correction factors and from the determination of the gamma-rays detection efficiencies. Moreover, indirect methods involve the measurement of the total electron capture from the various shells which require the assumption of the L/K ratio data and the relative contributions from higher shells. For low atomic number elements, in which region the total electron capture/β^+ measurements are more numerous, there exists a discrepancy of 10-20% between the experimental and the calculated L/K values (Fig. 1.).

In recent years there has been considerable

accumulation of data mainly on the total electron capture/β^+ branching ratios. Although the experimental and the calculated values are claimed to be in fair agreement, the possibility of a large systematic error in the experimental data cannot be ruled out in view of the difficulties stated above. This can be seen from a considerable scatter in the experimental results. This is particularly true when these data have been used for the evaluation of the Fierz interference term b, which is one of the main subject of concern here. For the determination of b it is highly desirable that the transition should be either pure Fermi or pure Gamow-Teller in order that the result on b could be interpreted. Only a few isotopes have been shown to be a pure transition. Therefore, reference will be restricted to those few cases which are precise and reliable, and the Fermi Gamow-Teller admixture is known.

Among the indirect measurements, the best results are of Sherr and Miller (1954) for the Gamow-Teller decay of Na^{22}. This isotope decays by electron capture and by β^+ emission predominantly to the 1.28 MeV level of Ne^{22} with a spin change of 1 and no parity change.

They used a coincidence arrangement with a scintillation counter to determine 1.28 MeV gamma-ray intensity and a 4π Geiger-Muller counter for the β^+ intensity. By these methods they deduced the value of total electron capture/β^+ ratio to be $0.110 \pm .006$. They compared this value with the theoretical value of 0.1135 and obtained the upper limit of the Fierz term b to be 6%, according to the notation adopted here (See eq. (20)).

Indirect measurements on the total electron capture/β^+ ratio for the pure Gamow-Teller radiator Co^{58} have been done by several workers. Their values are listed in Table I and vary between 5.48 and 6.7.

Table I

Author	Total electron capture/β^+ ratio
Good et al (1946)	5.8 ± 0.2
Cook and Tomnovec (1956)	5.9 ± 0.2
Grace et al (1956)	6.7 ± 1.3
Konijn et al (1958)	5.67 ± 0.16
Ramaswamy (1959)	5.48 ± 0.25

The recent theoretical K-capture/β^+ value for Co^{58} by Nguyen-Khac (See Depommier et al. (1960)) with second order correction is 4.87. Previous value by Perlman et al (1958) was 5.2. The upper limit of the Fierz interference term has been quoted by Konijn et al and by Ramaswamy as 5.2 and 3.6 respectively in the notation adopted here (See eq. (20)). The theoretical L/K-capture ratio from Brysk and Rose's graphs (1955,1958) is 0.092. The experimental value by Mollier (1961) with wall-less internal source proportional counter is 0.108 $\pm$ 0.004. Therefore, the b value would alter depending on the adoption of theoretical or experimental value on L/K-capture ratio.

Direct measurements by a wall-less proportional counter and an internal gaseous source have been done by Drever et al (1956) and by Scobie and Lewis (1957). Drever et al obtained a value of 0.030 $\pm$ 0.002 for the K-capture/β^+ ratio for the Gamow-teller decay F^{18}. Comparing this result with the theoretical value of 0.0295 they obtained the upper limit of b to be about 5%. Scobie and Lewis, by means of similar technique, obtained K-capture/β^+ ratio to be $(1.9 \pm 0.3) \times 10^{-3}$

for the predominant Fermi transition C^{11}. They assumed the value of Drever et al for the Gamow-Teller contribution and comparing the experimental value with the theoretical value of K-capture/β^+ ratio of 2.0×10^{-3}, deduced b for Fermi transition to be less than about 20%. These measurements are free from the corrections arising from the source scattering, assessment of detection efficiency and uncertainty in the L/K data. The main difficulties in these measurements are the determination of the total K-capture events under the K-peak and the estimation of the background effects.

The limit on Fierz interference term obtained from the beta spectrum shape are not as well defined as those obtained from the K-capture/β^+ ratio measurements. These are reviewed by Wu (Siegbahn 1955) and by Konopinski (1957). For pure Fermi transitions the lifetime work of Sherr and Gerhart (1956) could be referred.

Thus it has been shown that the situation in the experimental field for the measurements of L/K-capture ratios seems to be better than that for the assessment of b from the orbital-capture/β^+ ratio. But it should be noted that most of the reliable experiments on

L/K-capture ratios are confined to low atomic number elements ($Z \gtrsim 35$). Therefore, more work on middle and high Z-elements are desirable before the relevant theory could be verified. The work described in this thesis is an attempt to fill the gap, by means of a technique developed by the author. This technique was also used for the measurement of Fierz interference term for the pure Gamow-Teller decay of Co^{58}. The result is free from the main difficulty involved in an indirect method in the estimation of counter detection efficiency.

CHAPTER II

EXPERIMENTAL METHODS

It has been pointed out in the previous chapter that there exists a great interest in the experimental measurements of the L/K capture ratios for the middle and high atomic number elements, where the magnitude of electron wave functions are more accurately known and the experimental results are so scarce. In this region the K x-rays being of the order of 30 KeV or more the gaseous source proportional counter technique would not be suitable, as the majority of the x-rays would escape the counter even at high pressure and large counter dimension. For this reason the use of proportional counter technique has been restricted to $Z \leqslant 40$. On the other hand, internal source scintillation counter technique has several advantages and seems to be the appropriate method of investigation for the energy range of interest. Hence, a new type of internal source scintillation counter technique was developed which gave results free from surface effects and was successfully used in the determinations of the L/K capture ratios for the middle and high atomic number elements. In addition, this method was also

used for the measurement of K-capture/β^+ ratio. The utility of this technique has been found to be very wide and is discussed in Chapter VII.

The internal source scintillation counter technique consists of incorporating the radioactive source under study in a suitable scintillation crystal. This is achieved by growing a scintillation crystal containing a trace of the source. In this way the source is thoroughly dispersed in the sensitive volume of the detector which, for practical purposes, could be regarded as having zero thickness. Thus there is no source self absorption or scattering and by virtue of 4π geometry, the detection efficiency is 100%. The method was introduced by Scarff-Goldhaber et al (1951) and Bannerman et al (1951) and was used for a few specific nuclear problems. However, its potency has not been fully exploited especially for the study of low energy radiations consisting of Auger electrons. In view of this a thorough understanding of the performance, general utility and limitations of the internal source scintillation technique seemed desirable. In the course of these investigations it was envisaged that the

undesirable escape correction could be eliminated by employing an improved well-type method. Throughout the work described here thallium activated sodium iodide scintillator was used as this is the most efficient phosphor as regards maximum light output per quantum of energy absorbed and shows a linearity of response for electron energy from 1 KeV to 6 MeV (Tayler et al 1951, and West et al 1951).

Well-type Method.

The improved internal source scintillation counter technique developed here is illustrated in figure 2. This method was developed initially for the measurement of electron capture studies and later extended for the studies of beta-decay process in general. The inner NaI(Tl) crystal was grown with the radioactive source under investigation. This crystal size was usually of the order of 5 mm diam x 5 mm and was cut, cleaned and polished from a grown crystal of size about 1 cm diam x $1\frac{1}{2}$ cm. The outer crystal was supplied by Nuclear Enterprise (Edinburgh) and the crystal size varied from $\frac{1}{2}$" cube to 2 cm cube. The well could be readily made with an ordinary hand drill and expanded

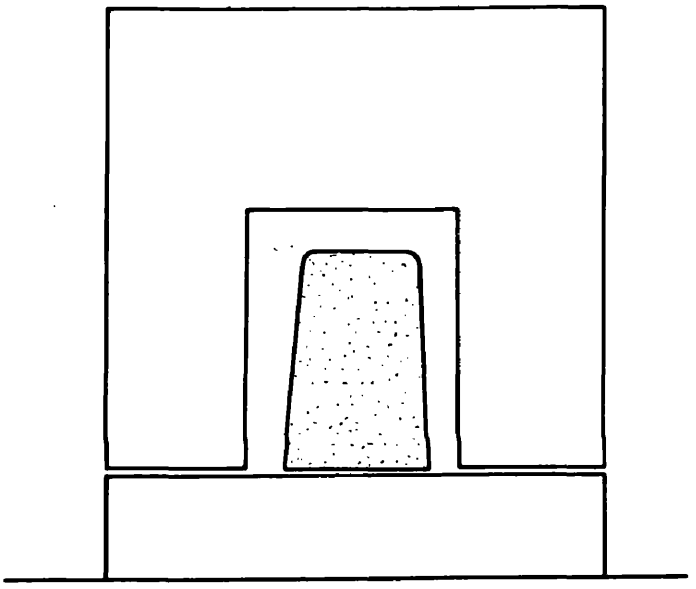

Fig. 2.

Well-type method which eliminates escape correction: The inner crystal is grown with a trace of the radioactive source and enclosed in an outer well crystal fitted with a lid.

by dissolving away in absolute alcohol. The drilling operation was carried out with the crystal covered with liquid paraffin. The lid was usually cut from the same crystal ignot and provided a close fit. The whole crystal assembly was immersed in liquid paraffin or mounted in dry air.

For the intermediate and the high atomic number elements the L-capture events consist of energies of about 5 KeV and 15 KeV radiations respectively corresponding to the binding energies of the daughter elements. These radiations comprise L x-rays or L-Auger electrons. In a crystal of size 5 mm^3 the L x-rays as well as the L-Auger electrons are completely absorbed. Similarly the K-Auger electrons are completely absorbed. But some of the K x-rays or the iodine x-rays associated with the detection process liberated near the surface layer of the active crystal, could escape. These later would be detected in the outer well-type crystal and the aggregate energy released by successive ionising radiations would be integrated and be registered as a K-capture event. No escape correction would therefore be necessary and

the L/K capture ratios follow directly from the relative intensity (counts) of the observed L- and K-peaks. Hence the results would not depend on the uncertainties regarding L- and K-fluorescence yields data and a knowledge of K_α x-ray group which if undetected would record as a spurious L-event. This method has proved to be simple, and effective in operation.

For the investigation of beta-spectra, it was necessary to mount the crystal in a dry air as the liquid paraffin enclosed between the active inner crystal and the well-type crystal could distort the beta-spectrum. This could arise from the partial loss of energy in the intervening paraffin of the escaping beta particles before being detected in the outer crystal. A dry box was used for mounting the crystal assembly. It was necessary to leave the crystals and the necessary accessories in a dry box over a period of about 1 to 2 days before being assembled. Phosphorous pentoxide was used as a drying agent and the air was circulated by means of a fan fitted inside the dry box. However, it was found that the arrangement with paraffin made little difference when the inner

crystal fitted closely inside the well (cf Ch. V p. 82)

Crystal Growing.

Single crystals of NaI(Tl) were grown by Bridgman method (1925). This method, shown schematically in figure 3, illustrates most of the principles involved in growing single crystals by solidification. A thin walled ($\sim$ 1 mm)satin-surfaced fused silica tube obtained from the Thermal Syndicate Ltd., Great Britain, was used for growing crystals. The internal diameter was about 1 cm and length about 1 inch. A capillary was drawn at one end to allow for the formation of a seed crystal. A clear quartz tube about $\frac{1}{4}$" diam and 6 inches long was provided at the other end. Approximately 4 to 5 gms of thallium activated sodium iodide chips, procured from Nuclear Enterprise Ltd, were cut into small pieces by stiff valet-type razor blade, cleaned with absolute alcohol and dried by filter paper. Each of these pieces were touched with a radioactive source which was in a solution form and introduced in the quartz tube. Usually a drop of the source was used. The quartz tube was evacuated through a trap immersed in liquid oxygen. After evacuation which took about

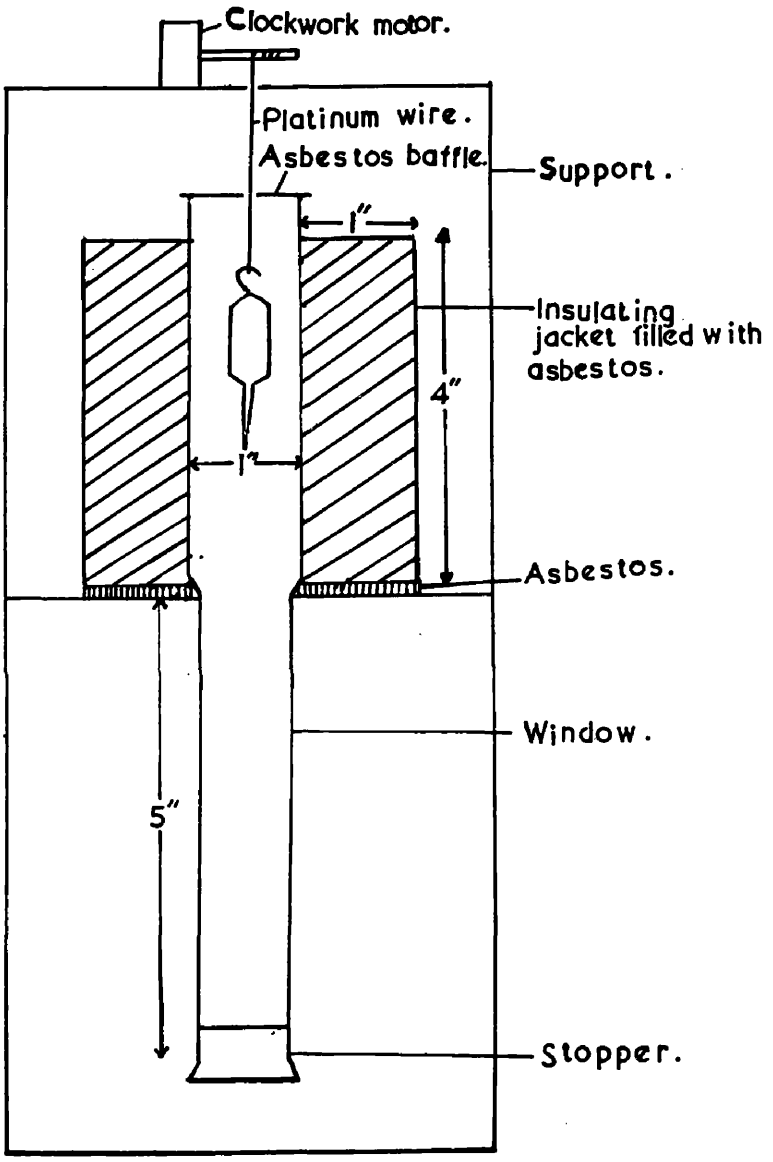

Fig. 3.

Schematic diagram of the vertical tube furnace used for growing crystals.

10 to 15 minutes the tube was slightly heated to drive off any water vapour and sealed off with oxygen flame while still under vacuum.

To produce a single crystal the quartz crucible was suspended by a platinum wire 0.002" diam in a vertical tube furnace. The central portion of about 2" in the middle of the furnace was maintained at 680°C with a temperature gradient of 40°C per inch. The inner diameter of the furnace was 1 inch with a bore thickness about $^{1}/_{16}$". 36 gauze nicrome wire was used as the heating element. The total number of turns was 56 covering a length of 4" of the tube furnace. To obtain adequate temperature gradient the spacing was kept closer in the central portion. The tube furnace was surrounded with asbestos to minimise heat loss. A clear glass tubing was cemented at the bottom end to permit observation. The crucible was slowly lowered ($\frac{1}{2}$" per hour) with a clockwork mechanism into a cooler zone. A seed crystal is first formed in the capillary and this continues to grow until all the liquid solidifies on it. A single crystal, the shape of the crucible, could be obtained. The whole

operation takes about 10 to 12 hours.

The difficulty most frequently encountered in the formation of a single crystal was due to the probability of multiple nucleation. This could be avoided by making a sharp point at the end of the capillary. Moreover, it was often observed that the crystals produced were rather imperfect, with large cracks and holes. This was particularly true when attempts were made to bring the temperature down rapdily. It was found desirable to allow about 5 to 6 hours for gradual cooling after the crystal has formed. This was achieved by stopping the clockwork when the crystal was grown and turning the volts off the variac, supplying current to the heating element of the furnace, in steps of 10 volts from 120 volt to 90 volts at intervals of 1 to $1\frac{1}{2}$ hr. Finally the furnace was switched off and left overnight to cool to room temperature.

Another requirement for growing good crystals was that absolute cleanliness should be exercised during the process of packing. In addition, the heating should not be applied before the crystal completely dried.

Crystal Cleaning and Mounting.

The crystal when ready could be taken out by cutting open the quartz crucible with a diamond saw. The crystal was washed several times with absolute alcohol to remove any source sticking on the surface. It could be cut in any required shape with a fine fret saw followed by rubbing down cut surfaces on waterproof silicon carbide paper, grade 400e. The whole procedure was handled under liquid paraffin. Finally the crystal was washed with absolute alcohol, treated with a buffer solvent of benzene to dissolve the alcohol remaining on the surface and transferred to several baths of liquid paraffin in succession. At all times touching the crystal by hand was avoided, and normally small tweezers were used for manipulation. The liquid paraffin usually contained air bubbles and it was desirable to drive it off by heating. The advantage of using several baths of paraffin was to remove any film of dissolved NaI in the solvent clinging on the surface which would turn the crystal yellow in a few minutes. In spite of all these precautions it was often observed that the crystal became cloudy or yellow

in a period of a few days. This would decrease the energy resolution. In such cases the crystal was recleaned before being used. The obvious disadvantage was the gradual dissolving away of the crystal.

At first the crystal was mounted in a glass container with a thin flat glass window cemented with 'Araldite'. It showed high phosphorescence effects in the region below 2 KeV and it was discarded in favour of an aluminium container with a thin mylar or glass window cemented with 'Bostik'. The crystal assembly was generally immersed in liquid paraffin and surrounded by aluminised mylar 0.001" thick. It was found subsequently that the Mgo reflector gives much better results. The optical contact between the crystal and the glass window was obtained by using a thin paint of silicone fluid between the glass window and the crystal surface. The liquid paraffin from the crystal surface was removed before packing with Mgo as this caused a loss of light resulting in the decrease of energy resolution.

Photomultiplier Consideration.

For the measurement of low energy radiation the

photomultiplier noise and the photo-cathode efficiency are of considerable importance, and in fact these are the main sources which limit the range of measurements. For these reasons an initial attempt to use a Du Mont 6292 phototube to analyse ~ 5 KeV Cs^{131} L-peak was not successful. Below 10 KeV the photomultiplier thermal noise was so severe that cooling the tube to freezing brine temperature was of little help. These difficulties were overcome by using the recently developed E.M.I. 9514S photomultiplier, which was specially made for low energy work. The thermal noise was considerably lower which made it possible to extend the measurements down to 5 KeV region. Moreover, the 'S' tubes are made with glass free from potassium, which contains the natural radioactive element K^{40}.

Figure 4 shows the schematic diagram of the cooling jacket used in the L/K capture ratio measurement for Cs^{131} described in Ch. III. Thermal equilibrium was obtained by maintaining the jacket at freezing brine temperature over a period of many hours. Dry ice (solid Co_2) was used to freeze the brine. Figure 5 shows the reduction in the photomultiplier thermal noise

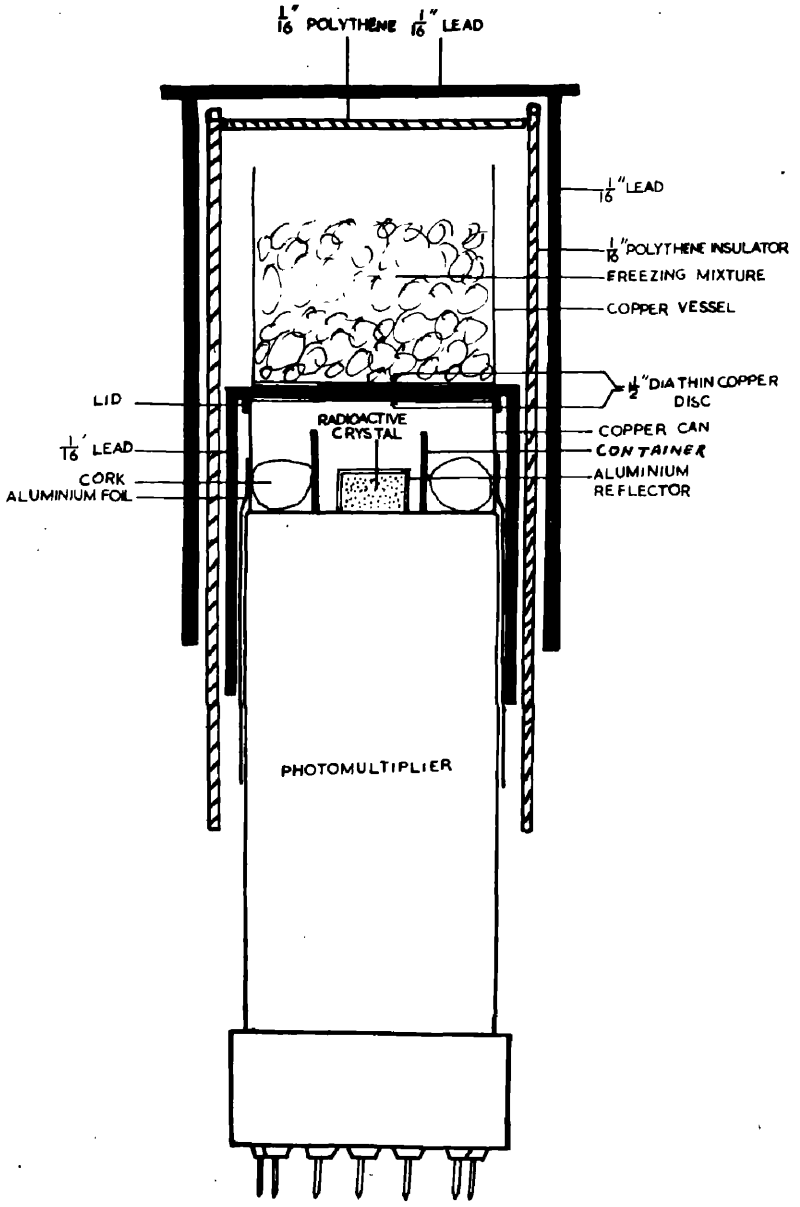

Fig. 4.

Arrangement for cooling the multiplier used for Cs^{131} experiment.

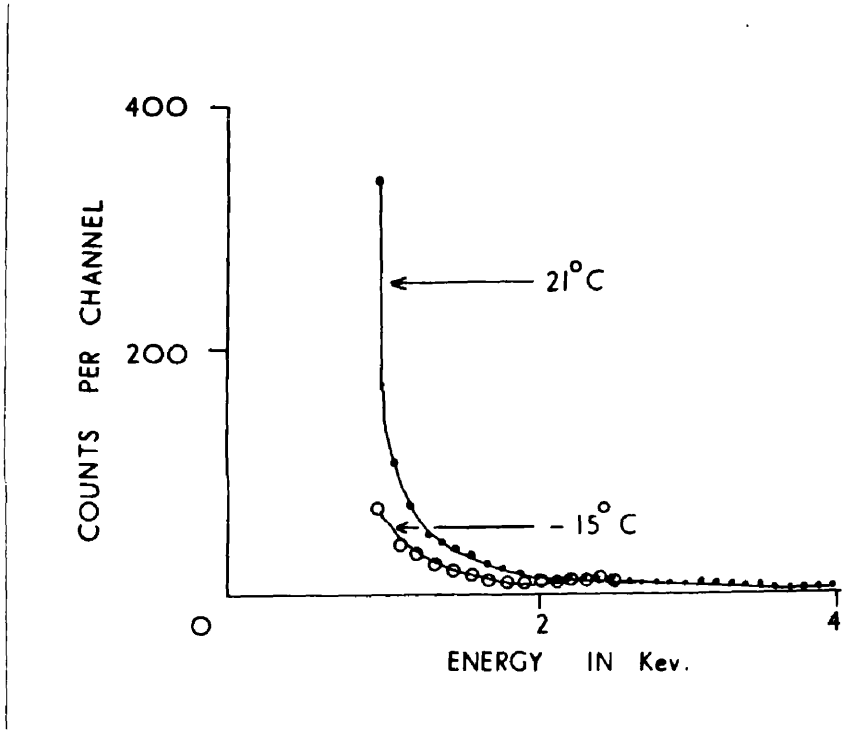

Fig. 5.

Reduction in the photomultiplier (E.M.I. 9514S) thermal noise by cooling.

from the room temperature of 21°C to the -15°C. Above 2 KeV the noise was very small and differed little when the tube was cooled. However, in the use of recent improved photomultiplier, the cooling was not necessary because the noise was practically negligible.

The Operation of the Well-type Method.

Figure 6 shows the K-peak of Cs^{131} obtained with the inner radioactive crystal alone. The peak with the crystal enclosed in the well-type outer crystal fitted with a lid is shown in figure 7. The energy resolution given by full width at half height in either case was about 33% for the K-peak and this indicated an excellent matching between the activated and the inactive well-type crystal. It was seen that the amount of the dissolved source in the crystal, which was of the order of less than about 0.1%,did not affect the relevant scintillation properties of the crystal.

Difficulties appeared in the assessment of the lower energy ends of the L-peaks for Cs^{131} and Ba^{131} and the K-peak for Co^{58}. For Cs^{131} and Ba^{131} the low energy rise persisted even after allowing for the background

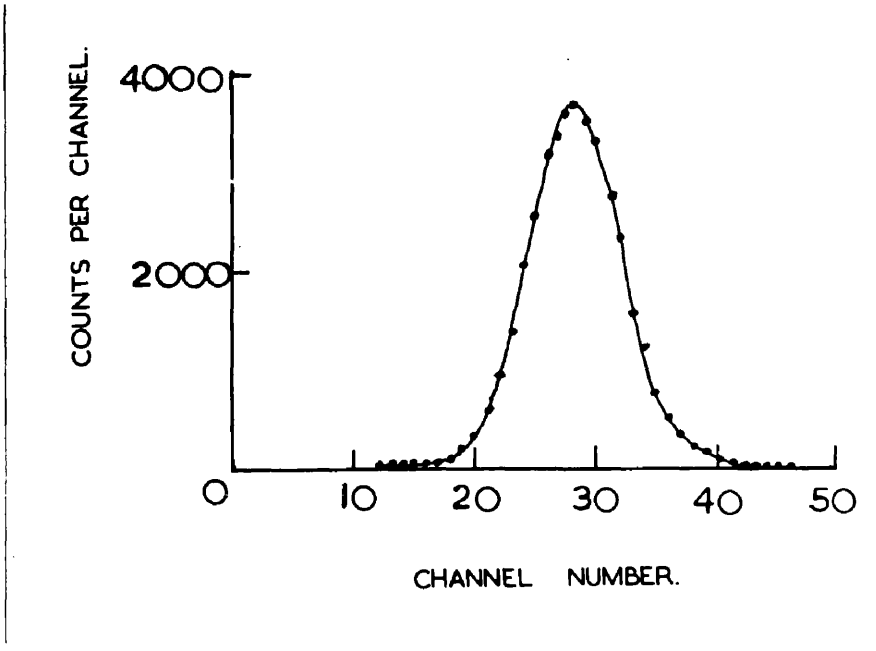

Fig. 6.

Cs^{131} K-peak with a NaI(Tl) crystal grown with the source.

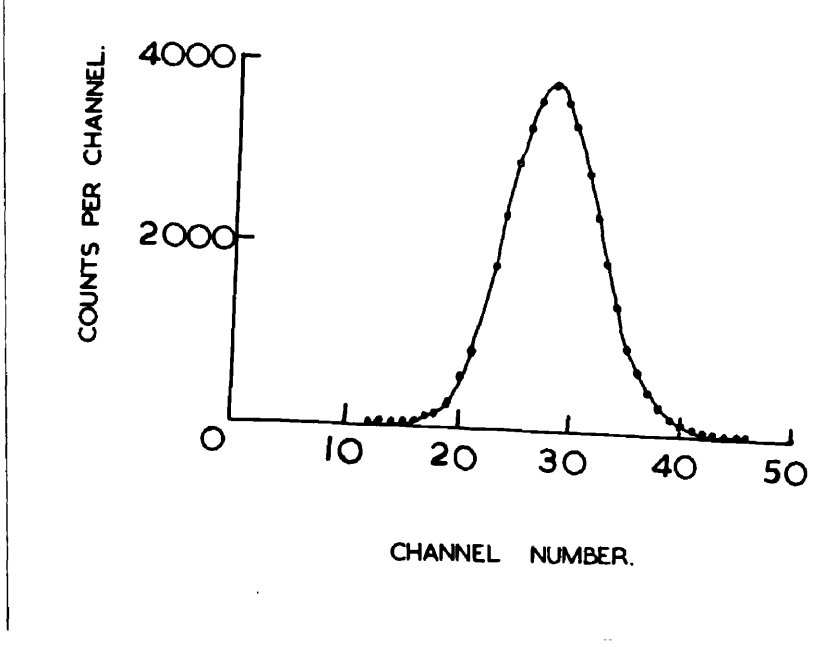

Fig. 7.

Cs^{131} K-peak with the active crystal enclosed in a well-type crystal fitted with a lid.

effects and this was attributed to the possible contribution from the M-capture events which would occur at about 1 KeV energy region. In view of this the curve was fitted with a statistical distribution (cf. W.B. Lewis 1942) assuming the K-peak as a standard. The validity of this assumption was further confirmed by a recent experiment on Co^{58} activated NaI(Tl) crystal with an E.M.I. 9514S photomultiplier having much improved photo-cathode efficiency (70μ amp/lumen). The Co^{58} K-peak is presented in figure 8 and shows the peak to valley ratio as 30/1. The K-peak with the previous 21μ amp/lumen multiplier is shown in figure 30.

Nature of Source Distribution.

In order to ensure the absence of possible surface effects the crystals were washed in absolute alcohol several times reducing its size from about 1 cm diam x $1\frac{1}{4}$ cm to about 5 mm^3. The crystals were washed from time to time even during the course of the experiments and the consistency of the results so obtained also confirmed the lack of source concentration near the surface of the crystals. Rough checks of the ratio

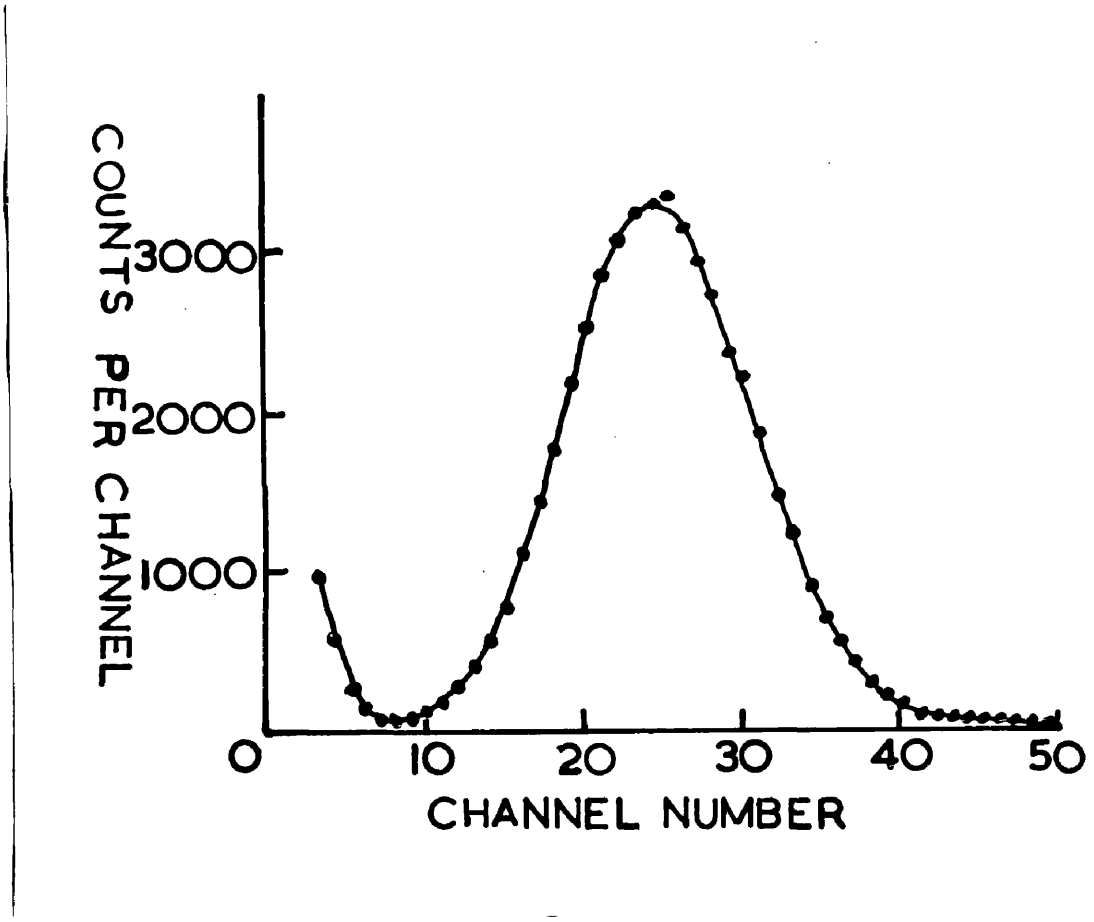

Fig. 8.

Co^{58} K-peak at 7 KeV obtained with an internal source in NaI(Tl) and an improved E.M.I. 9514S 70μ amp/lumen phototube.

of source counts to the amount of crystal could be made, this ratio remained constant.

To investigate the nature of source distribution inside the crystal, the Ba^{131} activated crystal was broken into four roughtly equal pieces and the counting rate under the K-peak was noted down against the weight of the crystal. This is shown in figure 9 and indicates that the source distribution was fairly uniform. The barium K x-ray energy being very near the iodine K absorption edge the Ba^{131} K x-rays in NaI(Tl) crystal would be mostly absorbed. However, the iodine x-rays, associated with the detection process, could escape from the edges of the crystal depending on the surface to volume ratio.

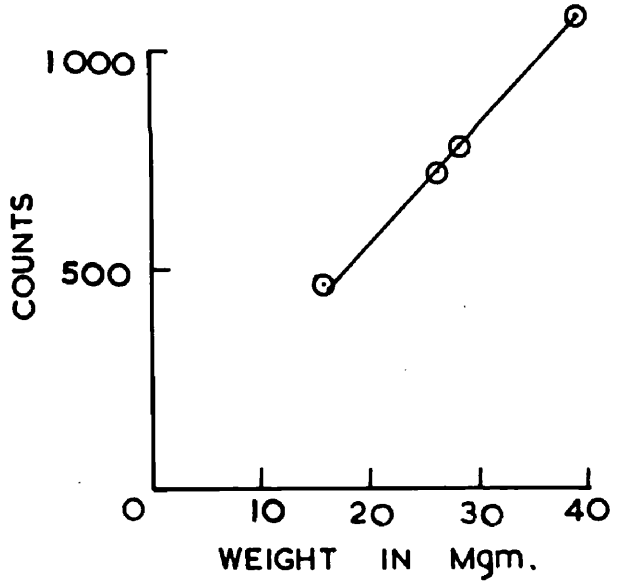

Fig. 9.

Examination of the source distribution in an activated crystal. The figure illustrates the Ba^{131} K-capture counts versus the weight of the crystal.

CHAPTER III

The L/K Capture Ratio in Cs^{131}.

1. Introduction

The isotope Cs^{131} possesses several features which make this very suitable for L/K capture measurements. Cs^{131} decays by pure electron capture, with a half life of 9.6 days (Yaffe et al. 1949), to the ground state of stable Xe^{131}. According to the nuclear shell model, the spin of the ground state of Cs^{131} is $d_{5/2}$. This value was confirmed experimentally by Goldhaber and Hill (1952). The ground state spin of Cs^{131} was measured by Bellamy and Smith (1953) and was found to be $d_{3/2}$. In terms of the two measured spins, the transition can be classified as obeying the selection rules $d_{5/2} \rightarrow d_{3/2}$, $\Delta I = 1$, no. These are the properties of allowed transition if Gamow-Teller selection rules are followed. Evidence for the allowed transition is further derived from the log ft value of 5.3. The decay scheme is shown in figure 10. The intensities of the L and K x-rays have been studied by Fink (1955).

The electron capture transition energy is known from the inner bremsstrahlung spectrum end-point to be 355 ± 10 KeV (Saraf 1954). This value has been further supported by the

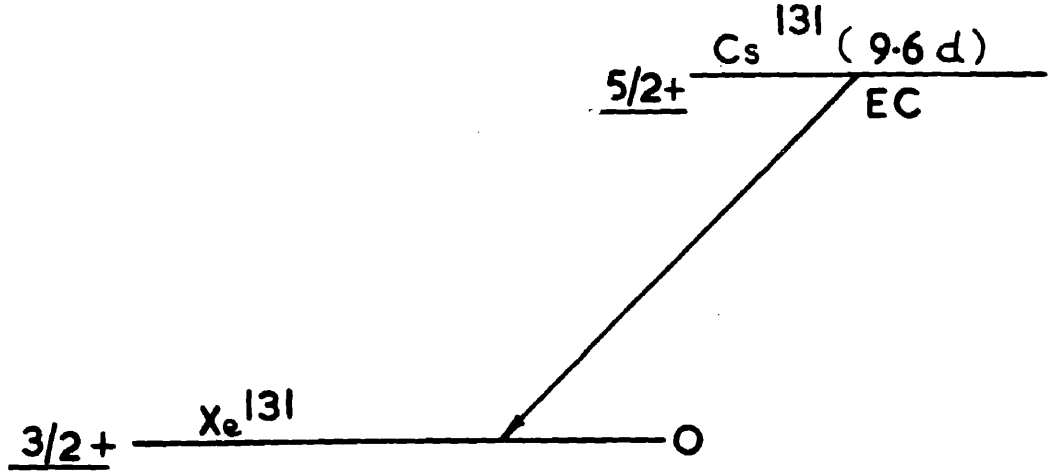

Fig. 10.

Decay Scheme of Cs^{131}.

subsequent measurement of the electron capture inner bremsstrahlung work of Hoppes and Hayward (353 ± 10 KeV) and Michalowicz (360 ± 15 KeV). With a value of 355 KeV for the transition energy, the theoretical L/K capture ratio was calculated at 0.145 from the Brysk and Rose's curves of the electron wave functions.

The L/K capture ratio had not been measured in Cs^{131} before the present work. The experimental measurements were mainly confined to low atomic number elements. Among a few more accurate cases, there existed discrepancies of the order of 10-20% more than the calculated value. It seemed desirable therefore to study the electron capture process further; and particularly for an intermediate Z nucleus. For such nuclei L/K values are very scarce. This direct measurement of the L/K capture ratio in a simple allowed decay of Cs^{131} provides, therefore, a critical check of the validity of the relevant theory.

2. Experimental Method.

Carrier free Cs^{131} was prepared chemically at Amersham Radiochemical Centre by separating the daughter nucleus of 12 day half-life Ba^{131} produced by an (n,γ) reaction on

natural $Ba(C0_3)_2$ at U.K.A.E.A., Harwell. It was obtained in solution form, dissolved in normal HCl solution, with a specific activity of about 2mc/ml.

To check the radiochemical purity of the sample, a thin source of the Cs^{131} was mounted between two pieces of $^1/_{16}$" thick perspex sheet. Using this as an external source a search was made for any gamma-emitting impurities in the source. A 2" diam x 2" NaI(Tl) Harshaw scintillator mounted on a Du Mont 6292 photomultiplier tube was used as a gamma-detector. A 1430A Dynatron pulse amplifier was employed and the spectrum was analysed in a C.D.C. transistorised multichannel pulse height selector. To minimise the room and cosmic-ray background effects the detector was shielded with 2" of lead shielding, provided with a 5 mm copper lining to absorb lead x-rays. The gain of the amplifier was adjusted to cover a wide energy range. Calibration was effected by external gamma-ray standard sources of Rad (46.5 KeV), Hg^{203} (279 KeV), Na^{22} (511 KeV and 1.277 MeV), Cs^{137} (662 KeV) and Co^{60} (1.173 and 1.333 MeV). Except for a very prominent clear photopeak at approximately 30 KeV, no line radiations were observed in the region of 10 KeV - 1 MeV, indicating that the source was very pure. The 30 KeV peak is due to the

predominant K_α x-rays following K-capture in Cs^{131}. Typical Cs^{131} K-peak with an external source as described above is shown in figure 11.

For the L/K capture measurement a few drops of the Cs^{131} source were diluted about ten times with distilled water and a thallium activated sodium iodide crystal was grown with one drop of the diluted source. The crystal, when grown, was first cleaned with absolute alcohol to dissolve away any Cs^{131} source sticking on the surface of the crystal. It was then treated with benzene to remove the absolute alcohol and finally immersed in liquid paraffin to keep it free from moisture. The crystal could be cut and cleaned as often as needed. Several similar crystals were grown.

Two series of experiments on the L/K capture ratio were done with separate sources. The first one was done without the well-type device and used single active grown crystals. The crystal sizes were approximately $6 \times 8 \times 3$ mm^3 and 7 mm diam x 1.0 cm. Both crystals were separately employed in the L/K ratio measurements. The crystal was mounted in liquid paraffin and surrounded by an aluminium coated mylar reflector of 0.002" thickness. A glass container with a thin glass window, cemented with

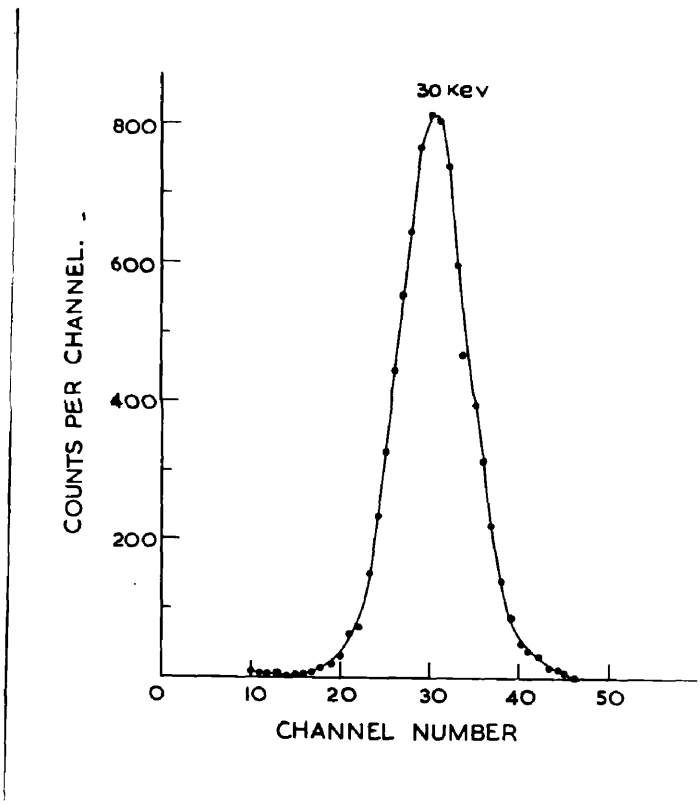

Fig. 11.

Cs^{131} K-peak with an external source.

Durofix or Araldite, was used. In view of the poor adhesive quality of Durofix and phosphorescence effects showed by Araldite, a thin mylar window stuck by Bostik cement to an aluminium container was used in the subsequent work.

It must be mentioned here that an initial attempt to observe the Cs^{131} L-peak ($\sim$ 5 KeV) with a Du Mont 6292 photomultiplier was unsuccessful. This was due to the photomultiplier noise in the low energy region arising from the thermal emission of electrons from the photo-cathode. Below 10 KeV the noise was so excessive that cooling the tube to freezing brine temperature ($-15^{o}C$) was not enough. This difficulty was overcome to a great extent by using low noise and high resolution R.C.A. 7265 and E.M.I. 9514S phototubes. The E.M.I. 9514S is especially suitable for low energy measurement because the tube has been made with potassium free glass. Naturally occurring potassium contains K^{40} which is a long lived radioactive source and could give rise to undesirable background. The E.M.I. 9514S tube was found superior to the R.C.A. 7265 from the noise considerations. The tube had been kept in the dark for a long period, and was not exposed at all during the experiments.

The L/K capture measurements with single active crystals were carried out with the R.C.A. 7265 photomultiplier. The photocathode and the crystal were cooled for several hours, in a cooling jacket, with freezing brine (-15°C). The system was surrounded by 2 in. thick lead shielding to minimise background effects. The pulses were amplified in a 1430A amplifier, inverted in an anode-follower and displayed on a C.D.C. multichannel pulse height analyser.

In the single crystal experiments it was necessary to assess the escape from the crystal edges of K_α x-rays. This could give rise to the detection of L x-rays in coincidence with K_α x-rays and thereby introduce errors in the L/K capture ratio. As K-capture is of the order of 7 times more frequent than L-capture, 1% escape of K_α x-rays would increase the result by about 7%. The x-ray escape correction can be calculated from absorption data. It seemed desirable, however, to measure this in a separate experiment. This was done by mounting the active crystal on top of a thin flat crystal (1.5 cm x 1.4 cm x 2 mm) with a thin aluminium sheet interposed in between. The spectrum thus obtained consists of K_α x-rays on the one hand and of K_β x-rays, or the iodine

K-escape x-rays associated with K_β x-rays on the other hand, it being impossible to resolve the latter K_β x-rays from the iodine x-rays. The K_β x-ray can, however, be expected largely to be converted into an I x-ray as the absorption coefficient for K_β x-rays in sodium codide is relatively very high. As a first order approximation the escape of K_β x-rays may be assumed to be zero ($\sim$2% of total K escape), I x-rays escaping instead. For the large crystal, which was cylindrical in form, the measurement was done by rotating the crystal through 90° each time. The solid angle presented in each case by the flat crystal was $^1/_3$ of the total solid angle due to the whole surface excluding the ends.

For the well type application, which gave results independent of the escape corrections in the L/K measurements, a single radioactive crystal grown with Cs^{131} was cut and cleaned to a size of approximately 5 mm^3. This was inserted in the well-type crystal of Harshaw NaI(Tl) which had an external size $1\frac{1}{4}$ cm^3, the walls of this latter were approximately 3 mm thick and was fitted with a lid 2 mm thick. The whole crystal assembly was mounted in liquid paraffin and 0.001" thick aluminised mylar reflector was used. An aluminium

container with a thin mylar window was used. The photomultiplier used was an E.M.I. 9514S tube. The pulses were amplified in a non-overloading amplifier (type NE 5202) and were displayed in a C.D.C. Kicksorter. The tube was kept in the dark for a long time to minimise the photomultiplier dark current. The tube was never exposed to any kind of light and the crystal mounting operation was carried out in complete darkness.

3. Results

The K- and L-peaks obtained with single active crystal spectroscopy will not be given here. However, the results will be presented and compared with the value obtained by the well-type method in the next section.

Typical K- and L-peaks obtained with the well-type method are shown in figure 12(a) and 12(b). By comparison with an external RaD (46.5 KeV) gamma-ray source the peaks were found to occur in the 35 KeV and 5 KeV regions, which correspond closely to the K- and L-shell binding energies of Xe^{131}. These figures show one of several runs in which the crystal and photomultiplier system had been cooled for several hours at -15°C with freezing brine. Data concerning the last 15 channels in figure 12(b) were

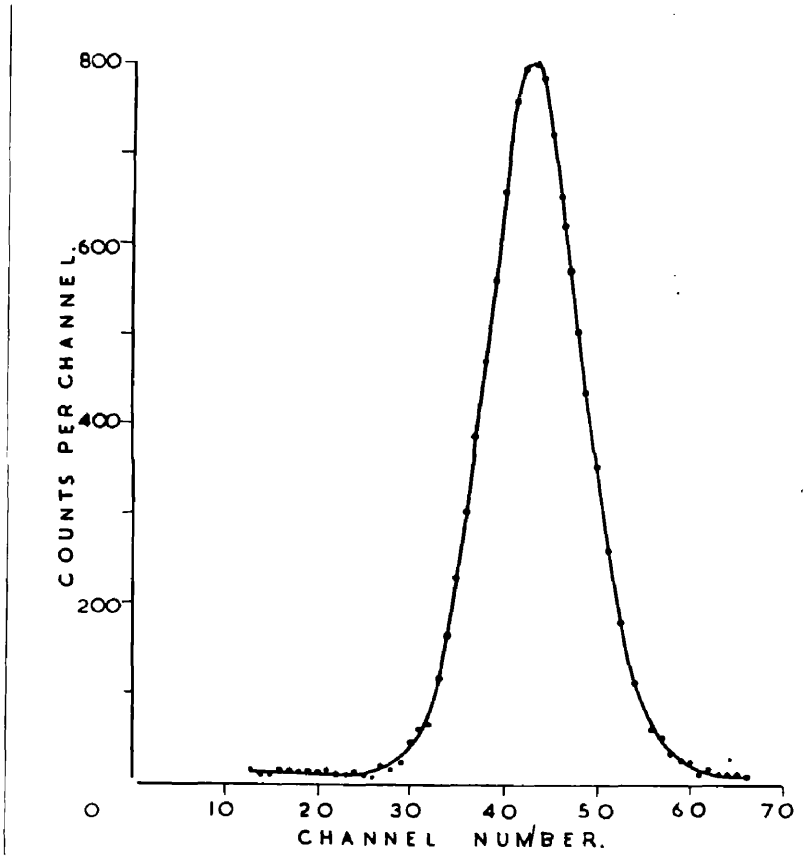

Fig. 12(a)

Cs^{131} K-peak at 35 KeV obtained by using the well-type method (5 min. run).

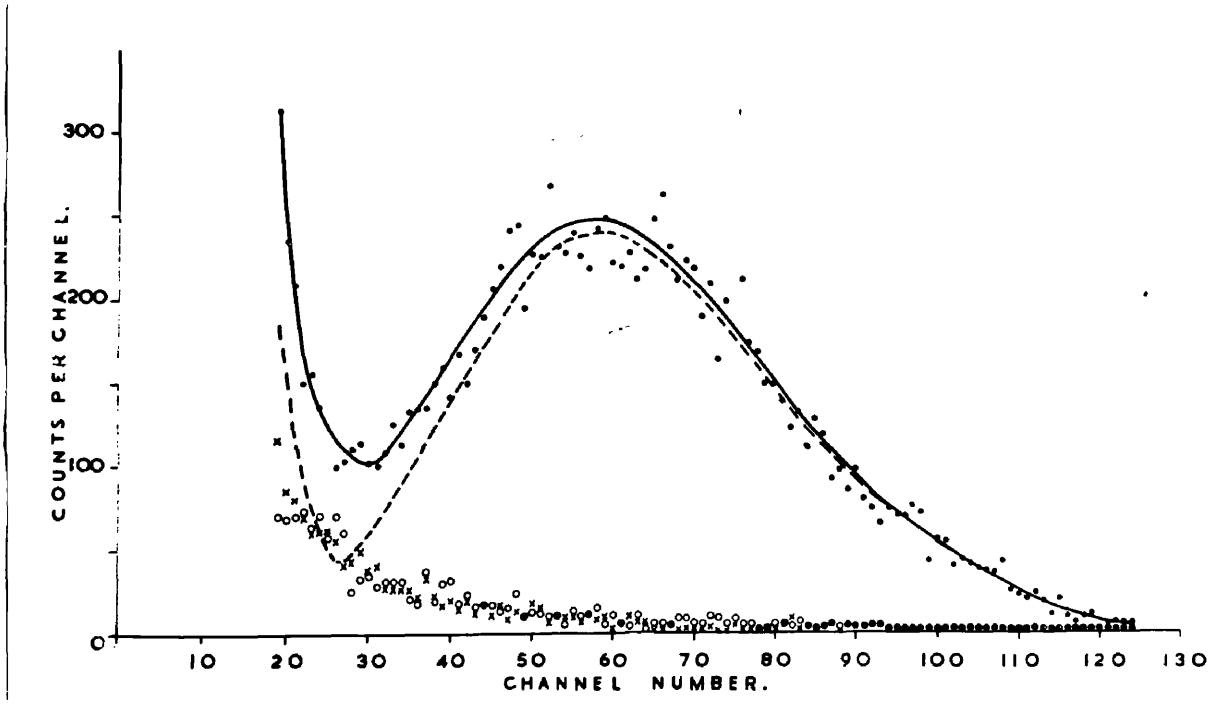

Fig. 12(b).

Cs^{131} L-peak at approximately 5 KeV obtained under the same conditions as the K-peak above. (30 min. run). Crosses show background run, taken with the well-type crystal alone under similar conditions; circles represent the thermal noise of the tube; the broken curve was obtained by allowing the background.

obtained in a subsidiary run. A background run was made with the well-type crystal alone, under identical conditions. The thermal noise of the tube was also measured similarly for comparison. Above 2 KeV the background curve differed little from the thermal noise curve.

In the region of the K peak background effects were small and figure 12(a) gives immediately the measure of K capture events. Figure 12(b) shows the L capture region and the broken curve shows the L-peak after background effects have been allowed for. Apart from the low energy rise this curve accords approximately with the distribution that could be expected from statistical considerations (of W.B. Lewis, 1942), taking the K peak as a standard. The rise at the low energy was found to be unaffected when the paralysis time of the kicksorter (35-200 μ sec) was increased, externally, to 1 m sec. The paralysis set up is shown in figure 13 . The paralysis pulse, which was a large (30V) negative square pulse, was generated in a pulse lengthener unit and could be varied between 500 μ sec and 1.3 m sec. The single channel kicksorter "window" was set at the K-peak. The paralysis pulse was delayed by 4 μ sec with respect to

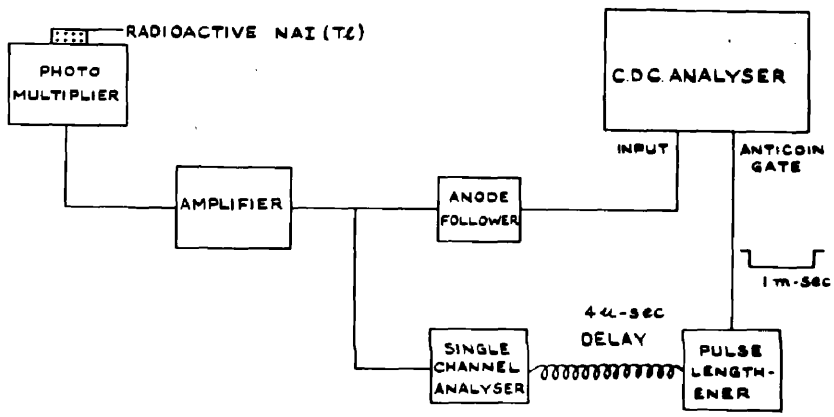

Fig. 13.

Paralysis set up used to check the phosphorescence effects.

the main pulse.

Moreover, a run on the L/K ratio taken after the crystals had been several days in the dark showed no essential change from figure 12, when allowance was made for the loss of source strength over that time. The rise, in a region associated with single electron emission from the photocathode, seemed to be induced by the L and K radiations which had already recorded properly in the L and K peaks. It could be due to delayed emission, for instance, induced by phosphorescence in the crystal and by glow in the multiplier. Such effects could be expected from the work of Harrison (1954) and Bernstein, Bjerknes and Steele (1958), for example. Further confirmation was obtained by wrapping a Cs^{131} source of comparable strength in $^{5}/_{1000}$" silver foil to stop the L x-rays and placing this in the well. The K peak occurred, with no L peak of course, but still quantitatively, the characteristic rise at low energy; indicating that the rise should be dissociated from the L-capture peak. In conclusion, it should be stated that M capture, which would give a broad peak of 1 KeV, could be contributing, at least partially, at the trough of the broken curve. The half-life of the Cs^{131} was found

by measuring the K-peak from one of the several crystals grown with the source. Measurement was carried out over a period of one month. The source was found to decay with $T_{\frac{1}{2}}$ = 9.6 days in agreement with the results of Yaffe et al quoted earlier. The results were shown in figure 14.

4. Analysis and Conclusion.

L and K capture events were analysed by measuring the relative areas under the L- and K-peaks. The kick-sorter dead time could be read directly in the meter and corrections for this have been applied. These were generally less than 1%. For analysing the L-peak the kicksorter bias was kept at 10 channels. Measurements were done repeatedly over several half-lives with similar results. The crystal was cleaned on many occasions with absolute alcohol and its size altered appreciably, the consistency of the results indicated that the source was distributed throughout the crystal. This was further confirmed by measurement of the amount of K-escape radiation, by surrounding the radioactive crystal with aluminium foil. The mean value obtained for the L/K capture ratio was 0.153 ± 0.008, and the error limits are

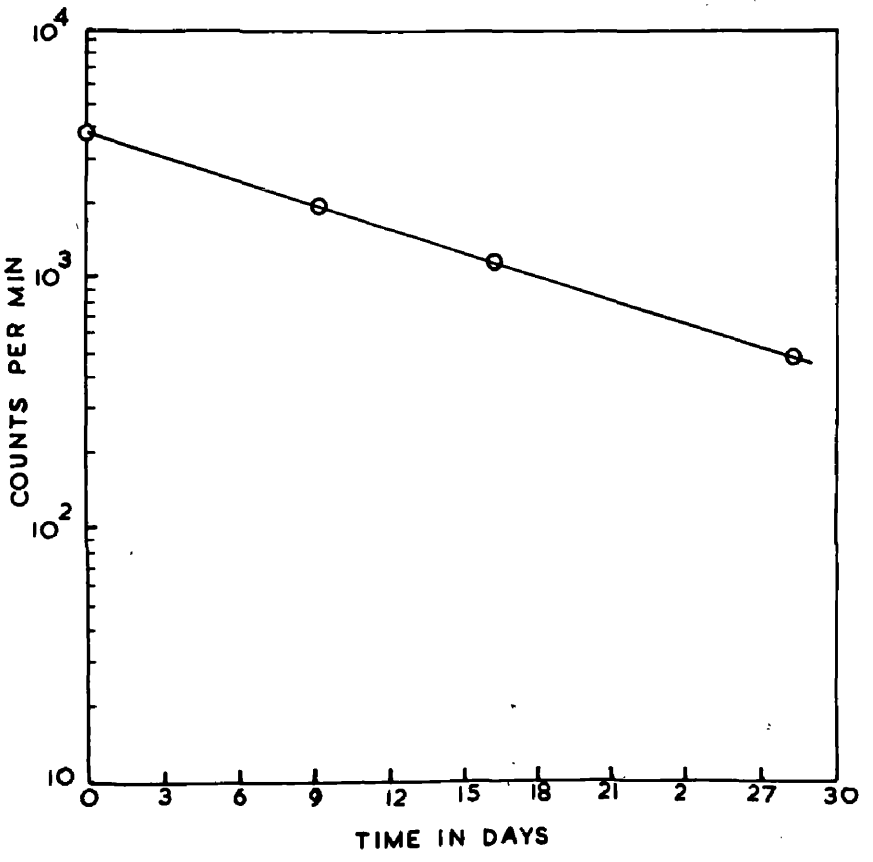

Fig. 14.

Exponential decay life time curve of Cs^{131}.

mostly associated with the assessment of the lower energy end of the L-peak. The statistical error of the measurement was less than 1%. It should be further stated, that if there is M capture present, in amount predicted by theory, then the L/K value will tend towards the lower limit.

The previous experiment with single active crystals and a different Cs^{131} source specimen gave values for the L/K capture ratio of approximately 16% in accord with the more precise value 0.153 ± 0.008 given above. The K x-ray escape was determined separately for both the crystals as described earlier and has been allowed for. The total fractional x-ray escape associated with the K-capture event was found to be approximately 5% for large crystal and approximately 9.5% for small crystal. The measured figure agreed with that calculated from absorption data assuming the source to be uniformly distributed throughout the crystal.

It should be mentioned here that in the first specimen of the source a very small peak due to the impurities was observed in the 14 KeV region but its intensity at the end of all the experiments was less than $1\frac{1}{2}\%$ of the source intensity. This would not affect the

L/K ratio values specified above. No other impurity radiations were observed. Experiments taken after the Cs^{131} had decayed showed that the impurity produces no contribution in the regions of interest. In the second source specimen no impurities were found.

In conclusion, the more accurate experimental value of the L/K capture ratio of 0.153 $\pm$ 0.008 is seen to be only marginally higher than the calculated value of 0.145 for this intermediate atomic number element Cs^{131}.

CHAPTER IV

The L/K-Capture Ratio in Ba^{131}

1. Introduction

The isotope Ba^{131} was shown to decay by electron capture to the excited levels of Cs^{131} by Katcoff (1947). The half life has been measured by several workers, the most recent value being 12 days by Wright et al (1957). Yu et al (1947) reported the absence of positrons in the Ba^{131} decay which was confirmed by Finkle (1947) using a magnetic deflection method. The decay scheme has been studied by many investigators. The information obtained up to 1958 is summarised in Nuclear Data Sheets (1958). The decay scheme proposed by Vartapetian (1956) is shown in figure 15 .

The shell model predicts a spin + $\frac{1}{2}$ for the ground state of Ba^{131}. So the transition from this state to the 620 KeV level involves a spin change of 1 and no parity change and is an allowed transition for which the theoretical L/K-capture ratio is independent of the nuclear matrix elements. It is a function of decay energy and electron distribution only (Ch.I. equ.(12)).

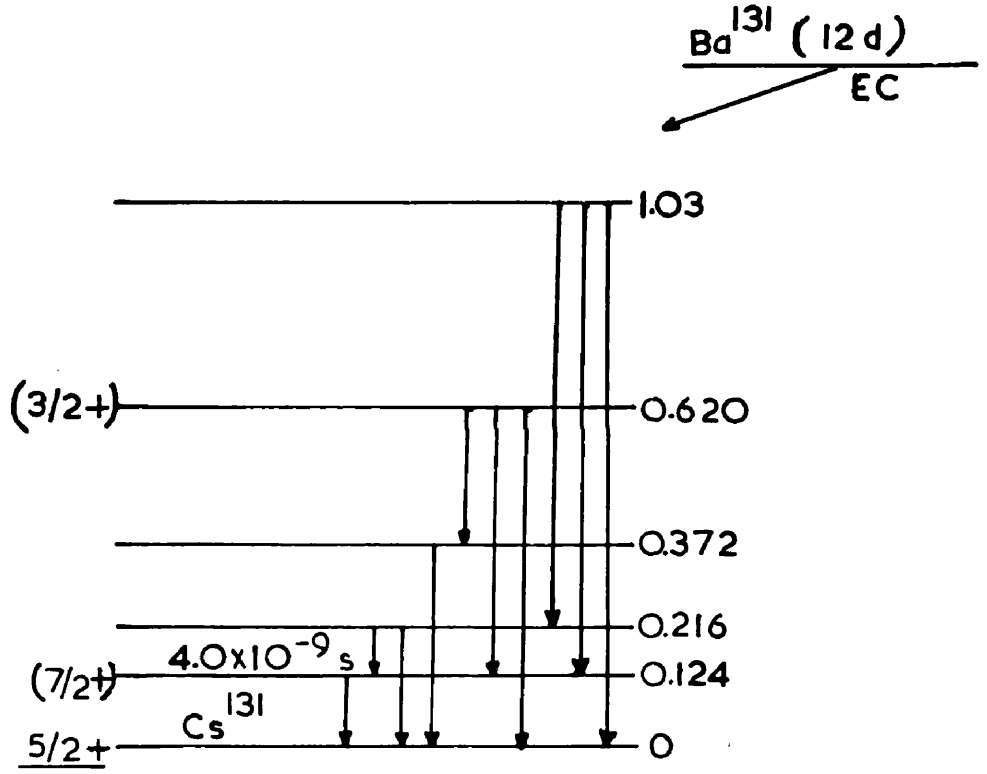

Fig. 15.

Decay scheme of Ba^{131}.

The energy available for the transition is not known. It was pointed out in Ch.I. that for high transition energies in which the K- and L-shell binding energies can be neglected, the theoretical L/K-capture ratio reduces to the approximate relation (15). As the transition energy associated with the 620 KeV level of Ba^{131} is more than 410 KeV, the experimental capture ratio obtained here could be compared with the calculated value based on the existence of a high transition energy. On the other hand, by inserting the experimental value in relation (12) of Ch.I, the transition energy can be evaluated.

2. Experimental Procedure

Ba^{131} was produced at U.K.A.E.A., Harwell by the $Ba^{130}(n,\gamma)Ba^{131}$ reaction on irradiating natural $Ba(C\theta_3)_2$ in a neutron beam. A high pile factor was used which gave a specific activity of approximately 80 μc/gm in one week. The other isotopes produced are Ba^{133}(2.5 yrs), Ba^{135m}(29 hrs), Ba^{139}(85 min) and Cs^{131}(daughter of Ba^{131}, 9.6 days).

The gamma-spectrum of Ba^{131} was studied with an

external source and a 2" diam x 2" NaI(Tl) crystal mounted on a Du Mont 6292 photomultiplier. The crystal was shielded with 2" of lead with a thin copper lining to minimise the effects of the cosmic and room background. A hundred-channel C.D.C. pulse height analyser was used for the recording of the spectrum. The gamma-ray spectrum, shown in figure 16 , exhibits prominent photopeaks at 86, 122, 216, 370, 495 KeV and a weak peak at 620 KeV. Figure 17, obtained with a higher gain, shows the Ba^{131} K-capture peak at 30 KeV corresponding to the predominant K_α x-rays. Calibration was effected with external RaD (46.5 KeV), Ce^{141} (142 KeV), Hg^{203} (279 KeV), Na^{22} (510 KeV), Cs^{137} (662 KeV) and Co^{60} (1.279 and 1.333 MeV) gamma-ray standard sources. A trace of Ba^{131}, mounted on thin mylar, was kept in close contact with a 1" diam x 1" NaI(Tl) crystal and the 496 KeV peak was noted down at regular intervals over a period of 3 weeks. The life time curve was plotted from the total number of counts under the peak. From this curve, shown in figure 18, the half life of the source was estimated to be approximately 12 days.

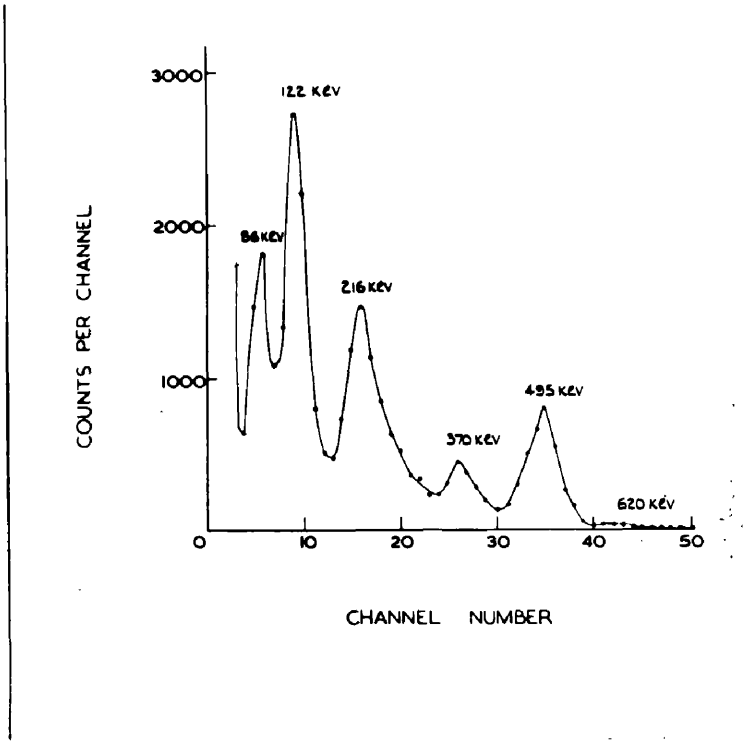

Fig. 16.

Ba^{131} gamma-ray spectrum in the 2" crystal with an external source.

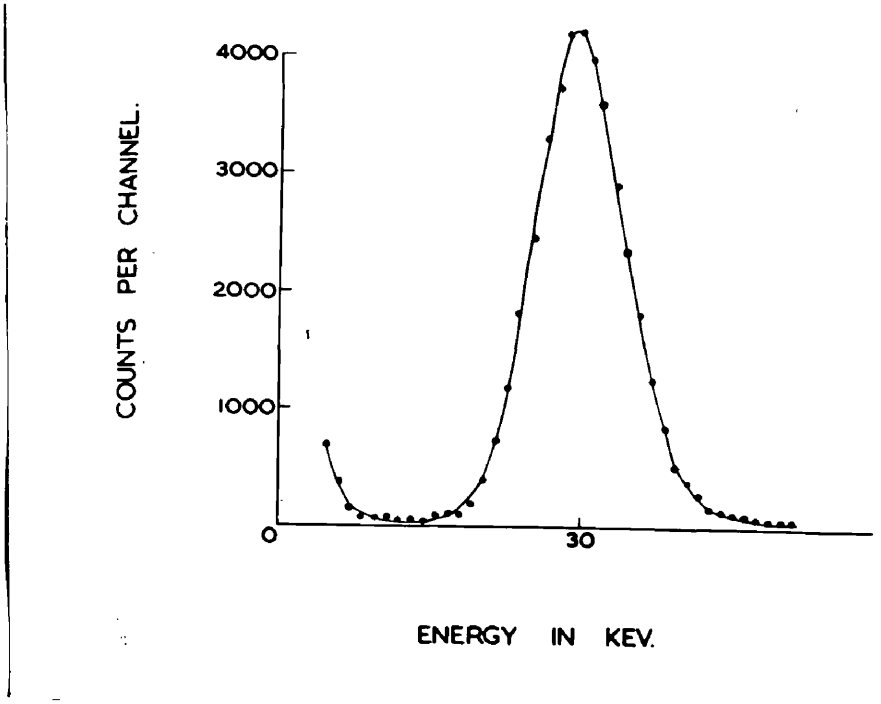

Fig. 17

Ba^{131} K-peak with an external source.

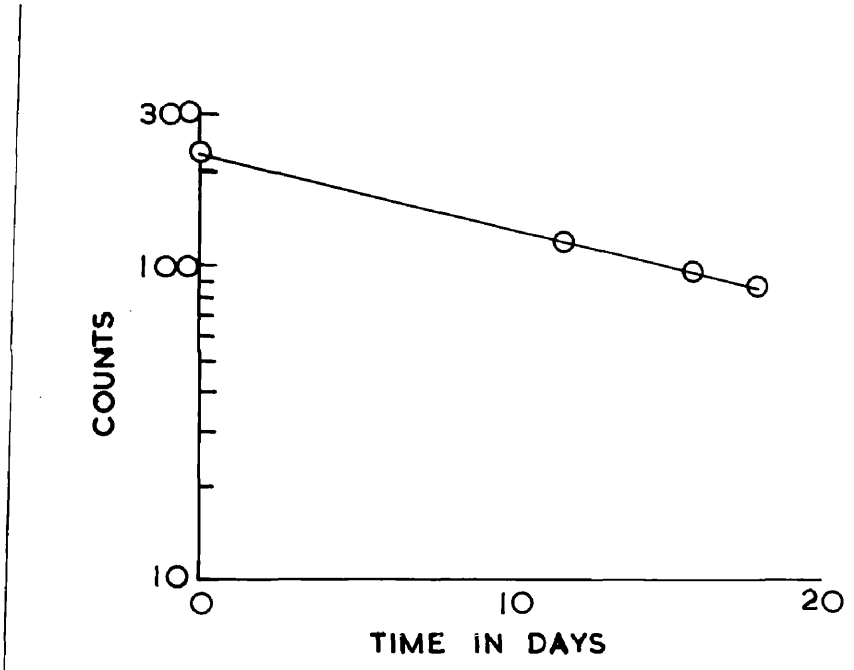

Fig. 18.

Exponential decay life time curve of Ba^{131}.

For the L/K-capture ratio measurement about 20 mg of the source was dissolved in 1 drop of concentrated nitric acid and diluted with distilled water. A scintillation crystal of thallium activated sodium iodide was grown with a trace of the source. Harshaw NaI(Tl) chippings were used. The experimental arrangement of the crystal assembly is illustrated in the inset of figure 21(a). The active crystal was cleaned with absolute alcohol, cut and polished to a size of 5 mm^3. This was completely enclosed by an outer well-type crystal fitted with a lid. The size of the outer crystal was $1\frac{1}{4}$ cm^3 with a central well of approximately 5 mm diam x 5 mm deep and the lid was 3 mm thick. The whole was immersed in liquid paraffin and was surrounded with 0.002" aluminised mylar reflector. The L-capture events which consist of L x-rays and L Auger electrons are completely absorbed in the inner active crystal. Similarly K Auger electrons are completely absorbed. However, some of the iodine x-rays associated with the detection process of the K x-rays, liberated near the surface of the active crystal, could escape from the inner crystal. The latter will

be detected in the outer, well-type crystal and renders any x-ray escape correction unnecessary.

The block diagram of the experimental arrangement is shown in figure. 19 . The active crystal assembly was mounted on an E.M.I. 9514S photomultiplier which was selected for its low thermal noise and good resolution. A Harshaw NaI(Tl) scintillator $1\frac{3}{4}$" diam x 2" was mounted on a Du Mont 6292 photomultiplier and was placed in close proximity with the main crystal assembly. To prevent any iodine escape x-rays from the 2" crystal being detected in the main crystal, $\frac{1}{2}$ mm thick lead sheet was provided in front of the 2" crystal. The main pulses were amplified in a N.E. 5202 non-blocking amplifier. Pulses from the 2" crystal triggered a single channel kicksorter (I.D.L.672A) with the "window" set at 496 KeV. The "window" setting could be effected by letting the single channel output to display its own spectrum. The position of this gamma-ray "window" is shown by the arrows in figure 20 . Amplified pulses from the main counter were fed into a discriminator. The output from the discriminator was delayed by 2 μ sec to allow for the internal delay of the single channel

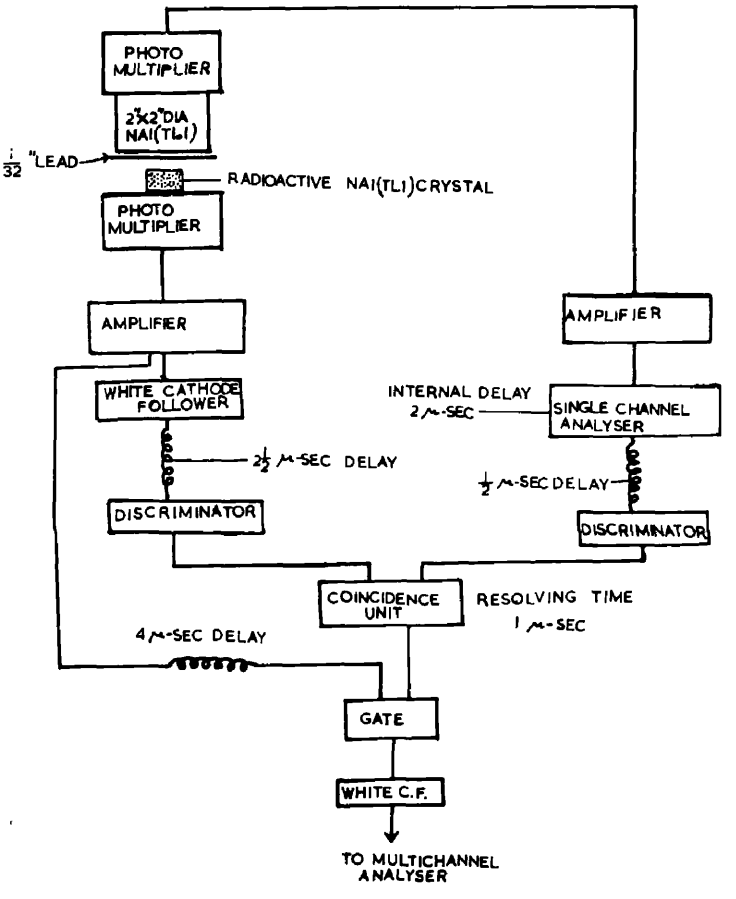

Fig. 19.

Block diagram of the electronic equipment for coincidence counts.

kicksorter output. A coincidence unit with a measured resolving time of 1.2 μ sec was used. This controlled a gate which generated a gating pulse of 10 μ sec. The K-and L-peaks were analysed by taking coincidences with the 496 KeV component from the 620 KeV transition. The highest energy gamma-rays associated with the electron capture decay of long-lived Ba^{133} is 360 KeV (Langevin 1956) and so would not interfere with the above results. The random coincidence rate was assessed by inserting an extra delay of $2\frac{1}{2}$ μ sec between the single channel kicksorter output and the input of the coincidence unit. The K and L-capture events were analysed in separate runs by changing the amplifier gain. A check on the stability of the system was made at regular intervals by ascertaining the counting rate from the "window" output of the single channel kicksorter and by allowing the gamma-gating pulse to display its own spectrum. No gain shifts were observed.

Figure 20 shows the gamma-ray spectrum from the 2" crystal in coincidence with the 36 KeV K-capture radiations in the source crystal.

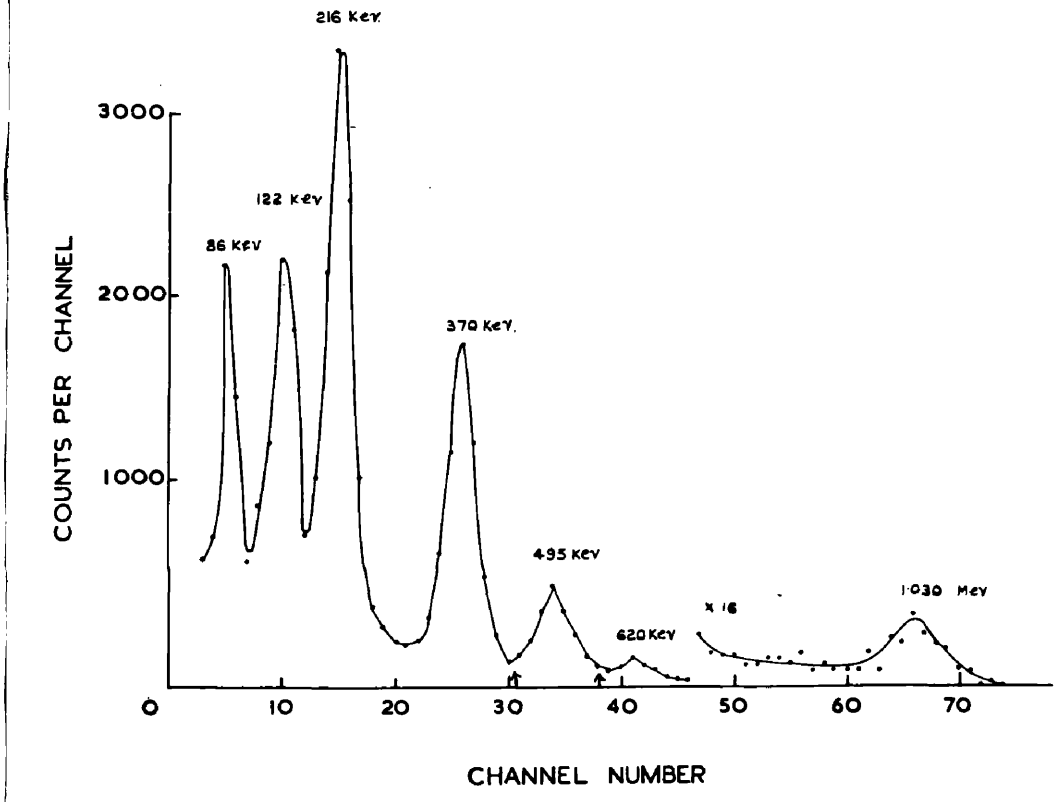

Fig. 20

Ba^{131} gamma-ray spectrum in the 2" crystal in coincidence with the K-capture radiations in the source crystal.

3. Results and Discussion.

Typical K-and L-capture peaks in coincidence with 496 KeV radiation are shown in figures 21(a) and 21(b) respectively. Under the K-peak the background effects were small. In figure 21(b) the solid curve shows the experimental points. The dashed curve has been obtained by subtracting the background shown by the crosses. The low energy end of the L-peak was established by fitting a statistical distribution (cf W.B. Lewis, 1942) taking the K-peak as standard. This could be expected from the scintillation response of the detector. Validity of this procedure was obtained from measurement of the K-capture peak of Co^{58} with an improved E.M.I. 9514S photomultiplier. This is discussed in detail above (Chapter II, page 52). The rise at the low energy region could be explained if M-capture occurs as expected.

The areas under the K-and L-peaks gave the total K-and L-capture events respectively. Several runs were taken which all showed consistent results. A mean of the values of L/K-capture ratio obtained from several runs was found to be 0.139 ± 0.008. Allowance

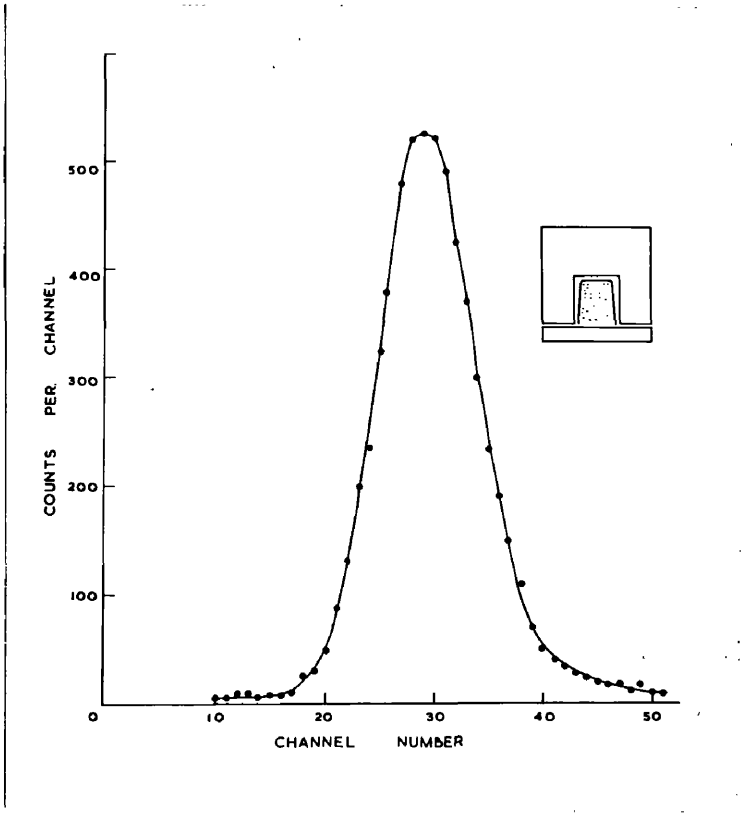

Fig. 21(a)

Ba^{131} K-peak at 36 KeV obtained by taking coincidence with 495 KeV gamma-rays (2 hr. run).

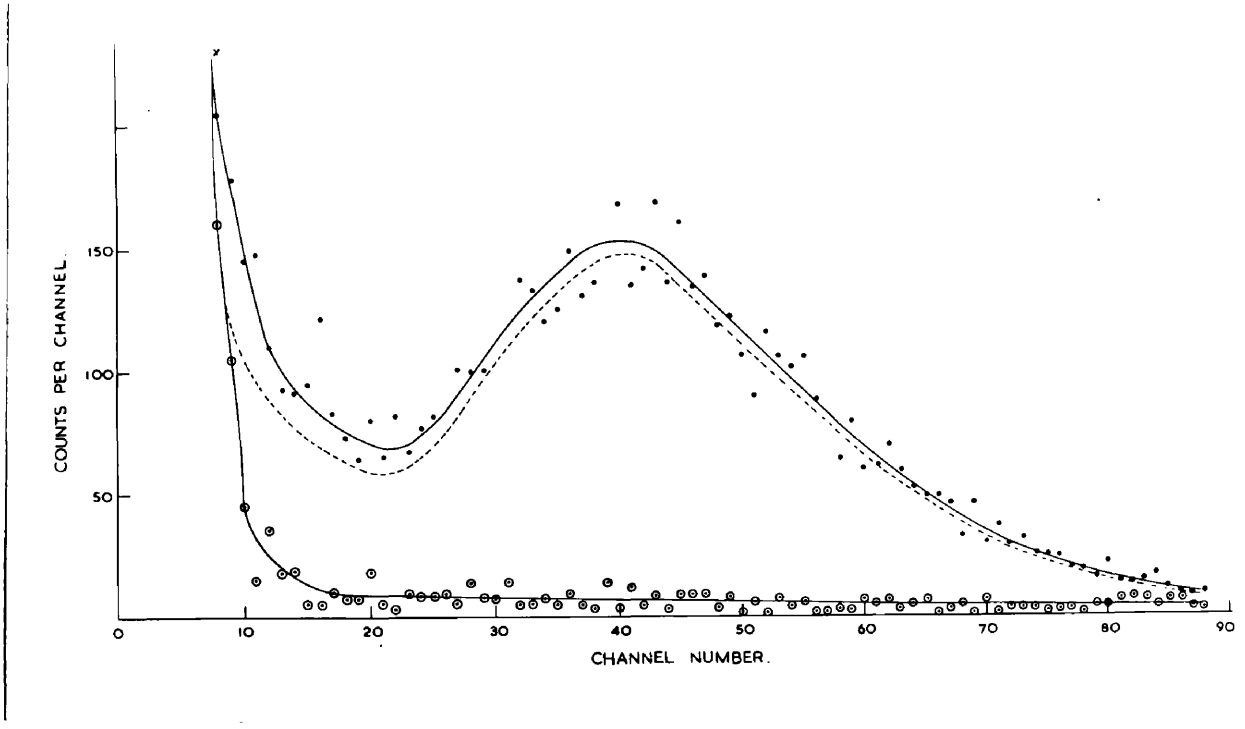

Fig. 21(b)

Ba^{131} L-peak at about 6 KeV obtained by taking coincidence as in Fig. 21(a). The lower curve shows the random coincidence rate. The broken curve represents the peak after deducting the random counts (12 hr. run).

has been made to take into account the finite decay of the source activity in the K-capture events. These were generally very small. The statistical error of the measurement was about 1%. The main error limit was associated with establishing the low energy end of the L-peak. This was estimated to be correct within 5%.

The experimental value of the L/K-capture ratio of 0.139 ± 0.008 can be compared with the calculated value of 0.124, based on the existence of a high transition energy corresponding to the transition to the 620 KeV state. On the other hand, by substituting the experimental value of 0.139 and the value of $\frac{g_{L_1}^2 + f_{L_{11}}}{g_L^2} = 0.124$ in eq. (12) of Ch. I, the electron capture transition energy to the 620 KeV level becomes 540 KeV. However, the error limit in the above experimental value of the capture ratio precludes an exact determination of the transition energy because of the insensitive nature of the capture ratio at high transition energy.

CHAPTER V

The L/K Capture Ratio and Beta-spectrum of Tl^{204}

1. Introduction.

The isotope Tl^{204} was known to decay by beta emission or, with a smaller probability, by electron capture according to the decay scheme shown in figure 22 after der Mateosian and Smith (1952). These authors further established that the decay processes are not accompanied by gamma-rays or internal conversion electrons, and so go directly to the ground states of each of the daughter nuclei. The most recent measurement on the half life by Fink and Robinson (1959) with proportional counter indicates a value of 3.78 ± 0.04 yrs. This value is in quantitative agreement with earlier values quoted in the literature. (Nuclear Data Sheets 1958). The inner bremsstrahlung spectral distribution associated with the electron capture processes was investiaged by Jung and Pool (1956). They used an external Tl^{204} source and obtained a value of 376 ± 20 KeV for the transition energy. Previous measurements on the transition energy by der Mateosian and Smith, referred to before, by internal source scintillation counter technique, yielded a value at approximately 335 KeV. The log ft value is 8.4 and indicates that the transition is a

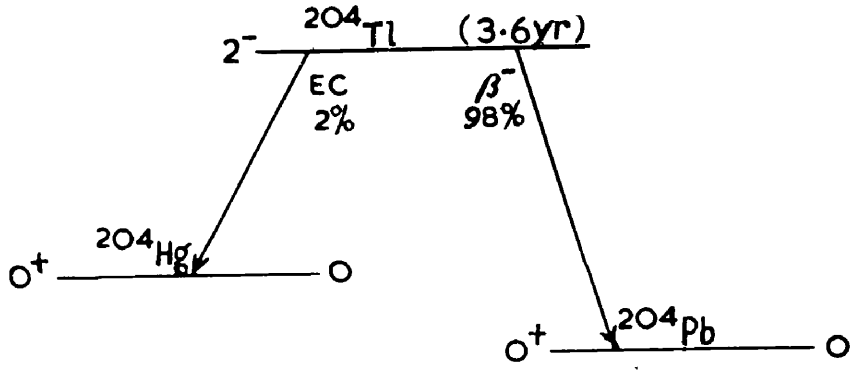

Fig. 22.

Decay Scheme of Tl^{204}.

unique first forbidden type.

From the nuclear shell model considerations the ground states of the even even nuclei $_{82}Pb^{204}$ and $_{80}Hg^{204}$ are characterised by parity + and spin 0. Evidence for the assignment of 2^- for the ground state of Tl^{204} is derived from the unique first forbidden shape of the beta spectrum as reported by Lidofsky, Macklin and Wu (1952) and by several others. (Nuclear Data Sheets, 1958). The electron capture decay, which involves a spin change of 2 and parity change, can therefore be classified as a unique first forbidden transition.

The weak K-capture branch ($\sim 2\%$) in Tl^{204}, which occurs at 83 KeV corresponding to the binding energy of Hg K-shell, was first observed by der Mateosian and Smith (1952). They measured the K-capture/β^- branching ratio and deduced the electron capture transition energy at 400 KeV in close agreement with the more accurate value of 376 $\pm$ 20 KeV referred to earlier.

The beta spectrum, investigated by Lidofsky, Macklin and Wu (1952) with a solenoid spectrometer, gave a value of 765 $\pm$ 10 KeV for the end point energy.

The Fermi-Kurie plot was shown to have an "S" shape, characteristic of "unique" first forbidden transitions. After treating the Fermi-Kurie plot with an exact shape correction factor, as given by Konopinski (See Siegbahn 1955, p. 305) and represented by equ.(31), in Chapter I, a linear plot was obtained down to 100 KeV (cf Wu (See Siegbahn 1955, p. 33)). Below 100 KeV the linear plot was found to deviate upwards and it was suggested that this deviation might be due to the finite source thickness. Recently Grard (1958) has studied the beta spectrum using a double focussing spectrometer down to 50 KeV. He has confirmed a straight Fermi-Kurie plot, after an exact shape correction, in the range investigated. Below 50 KeV he suggested the rising curve found by others is due to instrumental error.

The L/K capture ratio in Tl^{204} had not been measured before the present work. This being a "unique" transition the matrix elements in the theoretical capture ratio cancel out and the L/K ratio can be calculated from the electron capture transition energy. Moreover, the contribution from the L_{III} shell should be quite appreciable, which is favoured with low transition energy. Among

the high atomic number elements there existed no experimental data to provide a check of the theory. Before the theory of L/K capture can be used with full confidence, it seemed highly desirable to extend the measurements for high atomic number elements. In the course of these experiments, further information on the beta decay branch was obtained down to 10 KeV region.

2. Experimental Method.

The isotope Tl^{204} was produced by irradiating the natural thallium compound $TlNO_3$ in the neutron beam at U.K.A.E.A., Harwell by means of the $Tl^{203}(n,\gamma)Tl^{204}$ reaction. A pile factor of 12 was used. A small portion of the Tl^{204} was dissolved in distilled water and a source was made by mounting Tl^{204} in between two slabs of perspex. A preliminary examination of the purity of the sample was made. This was done with an external source of Tl^{204}, described above and a 2" diam x 2" NaI(Tl) Harshaw scintillator mounted on a Du Mont multiplier. Aluminium sheet about 5 mm thick was introduced between the source and the detector to remove beta particles. The detector was shielded with 2" of

lead provided with a thin copper lining to absorb Pb x-rays. Pulses from the multiplier were amplified and displayed in a C.D.C. multichannel pulse height analyser. The gain of the amplifier could be changed. Background effects were assessed under identical conditions. Except for a prominent peak at about 70 KeV, no gamma-ray lines were observed between this energy and 1 MeV. Calibrations were effected with gamma-ray standard sources., RaD (46.5 KeV), Ce^{141} (145 KeV), Hg^{203} (279 KeV), Na^{22} (510 KeV and 1.27 MeV), Cs^{137} (662 KeV) and Co^{60} (1.17 and 1.33 MeV). The 70 KeV peak was due to the predominant K_{α} x-rays following K-capture in Tl^{204}. It is shown in figure 23. The total gamma-radiations probability was estimated less than 0.15% of the total disintegration probability.

The experimental method for the measurement of K and L capture events is illustrated in figure 25. The inner crystal was grown from Harshaw NaI(Tl) chippings with a trace of Tl^{204} source. The active crystal was cut and polished to a size of approximately 6 mm diam x 6 mm. This fitted closely into the well-type Harshaw NaI(Tl) scintillator. This latter had an external size

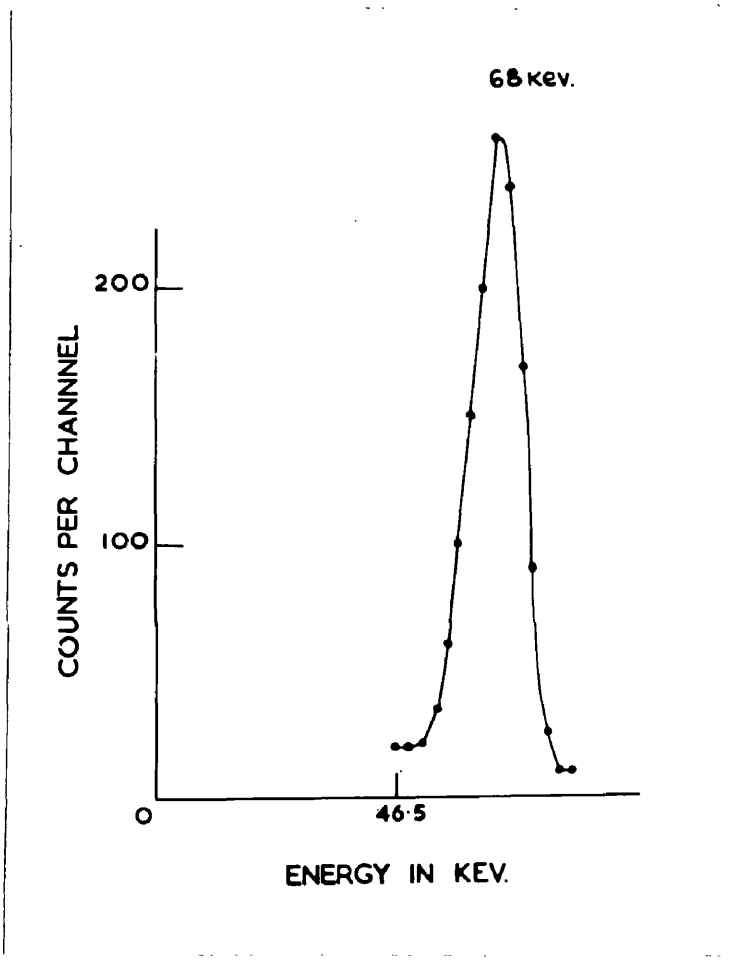

Fig. 23.

Tl^{204} K-peak with an external source.

of 2 cm^3 with a central well 6 mm diam x 6 mm deep and the whole was fitted with a lid 6 mm thick. This crystal assembly was immersed in liquid paraffin in an aluminium container having a thin mylar window and was surrounded with an aluminised mylar reflector of 0.002" thickness. An E.M.I. 9514S photomultiplier was employed. The photomultiplier was kept in dark over a period of nearly eight months and was never exposed to light.

The L events, which consist of L x-rays and L Auger electrons are completely absorbed in the inner active crystal. Some of the K x-rays, from K-capture events or the iodine x-rays associated with the detection process, may escape from the surface layers of the inner active crystal. As these will be absorbed in the outer well-type crystal and be recorded as simultaneous events, no x-ray escape correction is necessary.

To reduce the effects of cosmic ray and room backgrounds a preliminary check was made with the well-type crystal alone. The gain setting was the same as for the L and K capture measurements. A predominance of counts were observed in the 90-120 KeV region. Various grades shielding were tried. It was found

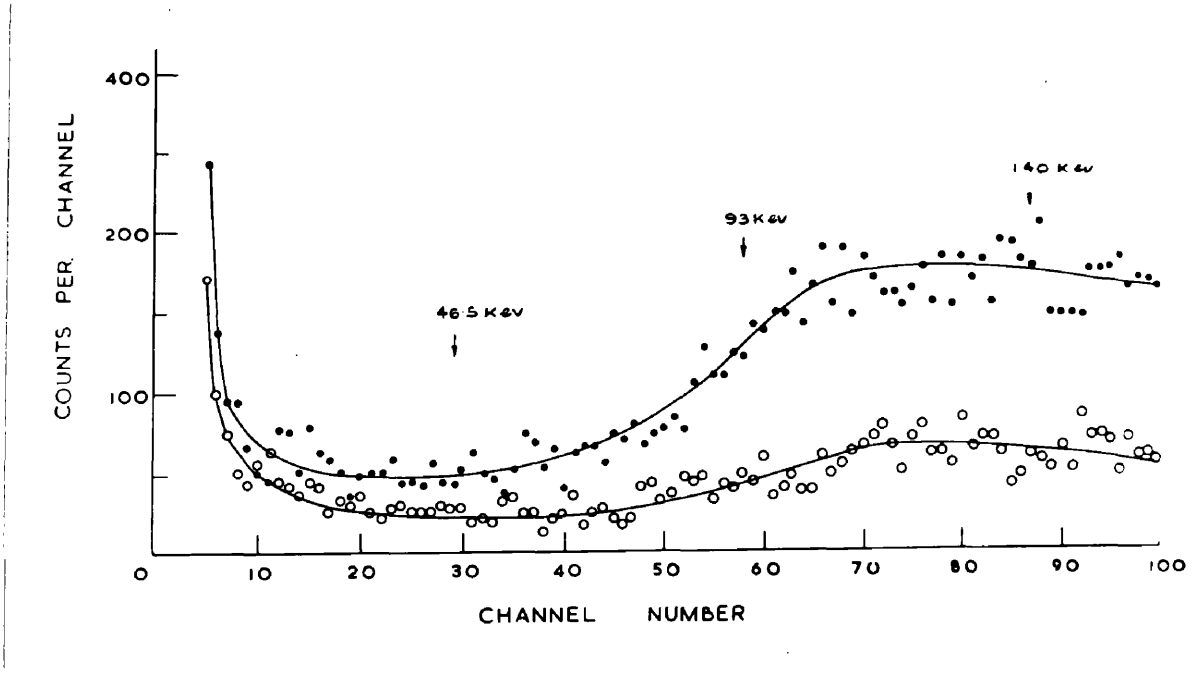

Fig. 24.

Background counts in the 2 cm^3 well-type crystal alone. The upper curve was obtained with a 2" Pb shielding and the lower with a 2" Pb provided with a graded lining of 1 cm iron and 3 mm copper (1 hr. run).

that 2" lead provided with a graded lining of 1 cm thick iron and 3 mm copper reduced the background effect considerably. This is shown in figure 24.

L- and K-peaks were analysed on a C.D.C. multi-channel pulse height analyser. Pulses were amplified in a N.E. 5202 non-blocking amplifier and inverted in an anode follower. All the measurements were carried out at the room temperature and this was noted down. Sharp peaks due to K and L-capture events at 83 KeV and about 14 KeV were observed by comparison with RaD external source (46.5 KeV and 15 KeV Pb x-rays. Typical K-and L-peaks superimposed on the continuous beta background, are shown in figure 25. Similar runs were made with the outer well-type crystal alone under identical conditions, to assess background effects. These were very small and are shown by crosses at the bottom of figure 25 .

The beta spectrum was analysed by lowering the gain of the amplifier and figure 26 shows the results so obtained. The small peak at the lower energy end is due to K-capture. Small background effects obtained with the well-type crystal alone are shown by crosses.

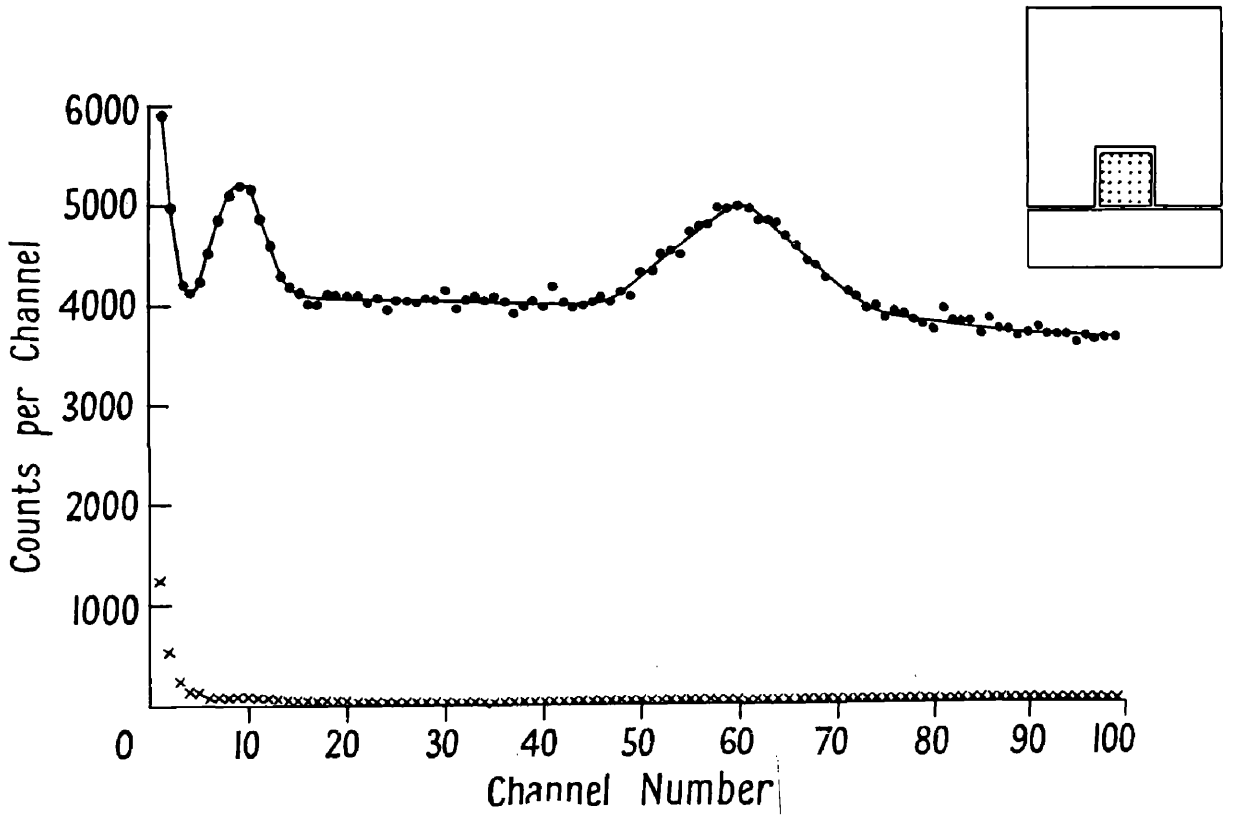

Fig. 25.

Tl^{204} L- and K-peaks superimposed on the continuous β^- background (2 hr. run). The background run, obtained under similar conditions from the well-type crystal alone, is shown by crosses.

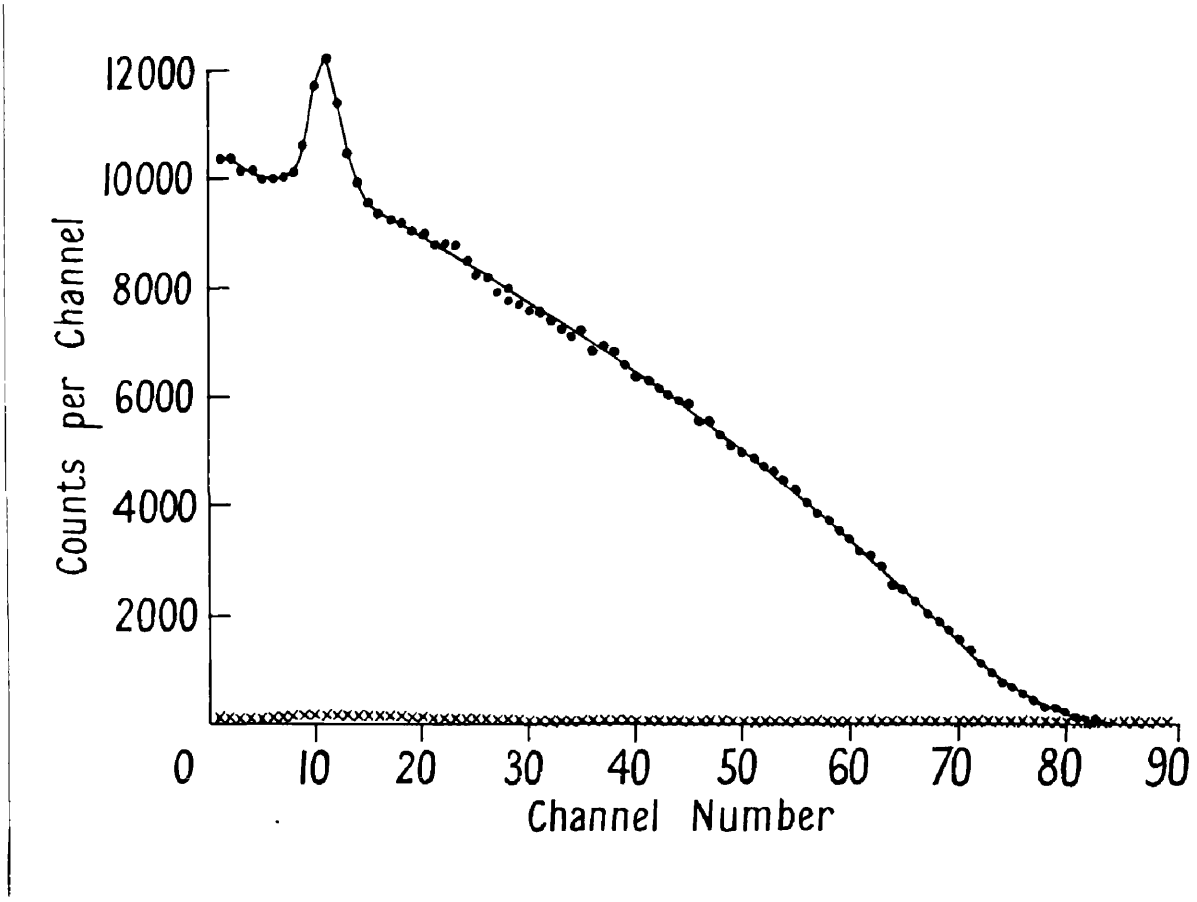

Fig. 26.

Tl^{204} β^- spectrum with a small K-peak superimposed at the low energy region (1 hr. run). Crosses show the background of the well-type crystal alone under similar conditions.

To obtain a quantitative measurement of the intensity of the beta spectrum, the crystal assembly was further mounted in dry air without liquid paraffin. This was done so that the high energy beta particles liberated at the surface of the inner crystal could reach the outer crystal without losing any of their energy in the intervening medium. The whole assembly was packed in magnesium oxide in a dry box. The small air gap between the inner active crystal and the well-type crystal could impair the light collection efficiency. A check was made with an external Tl^{204} source. The pulse height due to the dominant K_α line so obtained were compared with the height of the electron capture peak due to the inner crystal. The ratio of the heights were in close accord. This implies that the small air gap has no effect on the light collection efficiency.

Figure 27(a) and 27(b) shows the full Fermi-Kurie plot of the β^- spectrum down to 10 KeV after subtracting the K- and L-peaks, for the arrangement without paraffin. Some of the points at the low energy end were obtained from a subsidiary run with a higher gain.

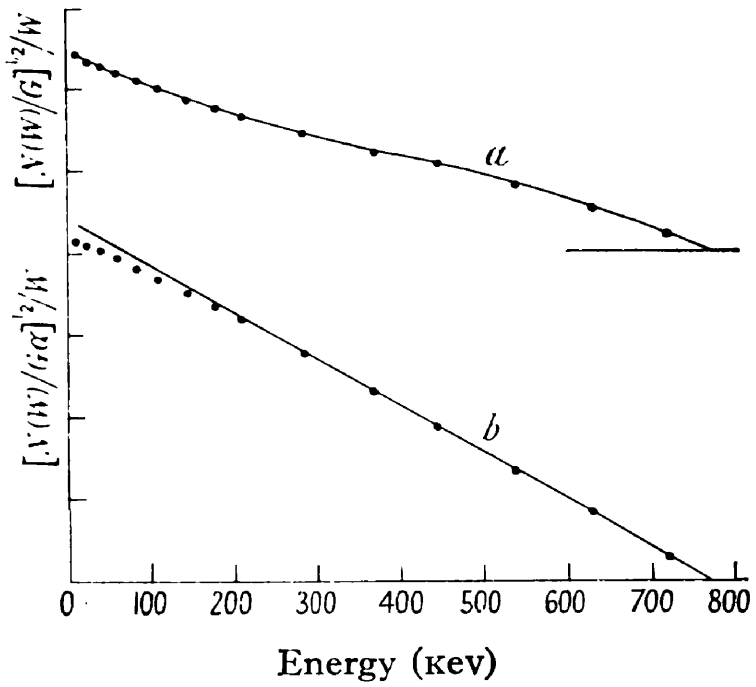

Fig. 27(a) S-shaped Tl^{204} Kurie plot obtained with the crystal assembly in dry air without paraffin.

Fig. 27(b) Tl^{204} Kurie plot of Fig. 27(a) corrected by the exact shape factor a.

After applying the exact shape correction factor given by the expression $\alpha = q^2 Lo(p-z) + 9L_1(p-z)$. (Chapter I, p.27) the plot of figure 27(b) was obtained. Here q is the neutrino energy and p is the electron momentum, Lo and L_1 are the tabulated functions of Rose, Perry and Dismuke. (See Siegbahn, 1955). This correction factor is discussed in detail in Chapter I.

3. Results and Discussion.

K and L events were analysed by measuring the relative number of counts under the K and L peaks. The beta background was assessed by drawing a smooth curve under the K and L peaks. Several runs were taken which were all consistent and a mean value of 0.42 ± 0.05 was obtained for the L/K capture ratio. The error limits are mainly associated with the assessment of the beta background.

The Fermi-Kurie plot of the beta spectrum given in figure 27, curve (a) shows the distinct "S" shape characteristic of first forbidden unique transitions. The data corrected by the exact shape factor is linear down to 220 KeV, and ends at 770 KeV. Below 220 KeV

the corrected plot deviated slightly downwards and not upwards from a straight line. The beta spectra shown in figure 27 are not corrected for the resolution of the instrument as this correction was found to be negligible in the range considered. The points in the figure are well clear of the L-and K-peaks so that the results are not influenced by them.

The K-capture/β^- ratio can be determined fairly accurately. The ratio is 0.0155 $\pm$ 0.001. This lies in the range $(1\frac{1}{2} \pm \frac{1}{2})\%$ obtained by der Mateosian and Smith (1952).

In conclusion, the experimental value of the L/K capture ratio of 0.42 $\pm$ 0.05 is in good agreement with the computed value of 0.45 $\pm$ 0.05 based on the electron capture transition energy, 376 $\pm$ 20 KeV. However, the earlier transition energy 335 KeV reported by der Mateosian and Smith (1952) yields a higher capture ratio 0.53. The L/K capture ratio obtained here is in close accord with the higher value for the transition energy.

CHAPTER VI

Determination of the Fierz Interference Term from the K-capture/Positron Ratio for the Pure Gamow-Teller Decay of Co^{58}.

1. Introduction

The positron spectrum of Co^{58} has been investigated by Deutsch and Elliot (1944), Strauch (1950) and Cheng et al (1952). These workers are in agreement on all features of the decay. They find the spectrum to be simple with an allowed shape and only one positron group. The Fermi-Kurie plots were shown to be linear with end point energies of 470 ± 15 KeV, approximately 470 KeV and 472 ± 6 KeV respectively. Later Cook et al (1955) reported a value of 485 ± 10 KeV for the end point energy. This value is rather doubtful as their results on the decay scheme were contradicted by subsequent measurements (Grace et al, 1956). More recently Daniels (1958) found a second positron component with an end point energy 1.28 MeV and relative intensity of about 0.6%.

The most recent measurement on the half life of Co^{58} was done by Schuman et al (1956) and is 71.3 days.

The log ft value is 6.59. The L/K capture ratio was measured recently by Moller (1961) with a wall-less proportional counter and a gaseous source and is 0.108 ± 0.004. The decay scheme of Co^{58} is shown in figure 28. after Frauenfelder et al (1956). This is in qualitative agreement with earlier work of Deutsch and Elliott (1946) and contradicts the results of Cook et al (1956), who obtained an additional 500 KeV gamma-component.

The spin assignment of the ground and first excited states of Fe^{58} is made on the nuclear alignment experiments of Daniels et al (1952). The spin of the ground state of Co^{58} has been confirmed recently by a paramagnetic resonance experiment by Dobrov and Jeffries (1957). The study of the weak branch through the 1.62 MeV state showed this state to be of spin 2 (Grace et al, 1956). The predominant decay which proceeds to the ground state of Fe^{58} through the 810 KeV first excited level by electron capture or positron emission involves a spin change of 1 and no parity change. These are the properties of an allowed transition obeying Gamow-Teller selection rules. This decay process has been shown to be principally Gamow-Teller by Daniels

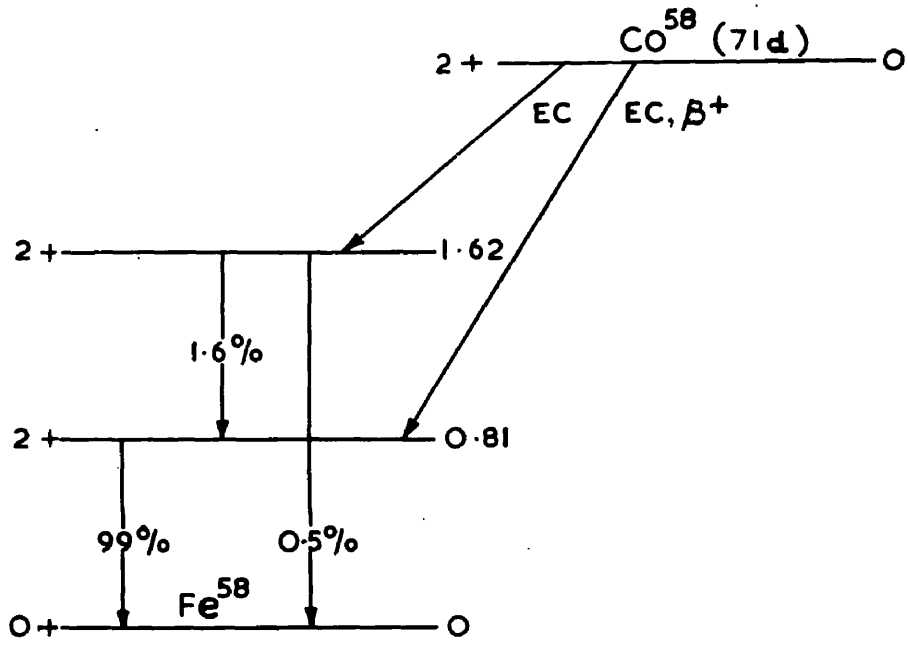

Fig. 28.

Decay scheme of Co^{58}.

et al (1952), Griffing and Wheatley (1956) and more recently by Dagley et al (1958) by nuclear alignment experiments. Dagley et al have considerably increased the experimental accuracy by using a more refined method. Unlike Griffing and Wheatley they used a single crystal for low temperature alignment and have shown that the beta-transition via the 810 KeV level to be pure Gamow-Teller with the Fermi admixture less than $\frac{1}{2}\%$.

The total electron capture/β^+ branching ratio of Co^{58} by an external source method has been reported by Good et al (1946), Grace et al (1956), Cook and Tomnovec (1956), Konijn et al (1958), and Ramaswamy (1959). These results vary between 5.5 and 6.7 (p36) In these indirect measurements, there exist uncertainties of many per cent, as there are difficulties associated with the assessment of gamma-ray detection efficiency and source strength. Moreover, in their adaptation to the determination of the Fierz Term b, knowledge of the L/K capture ratio is generally required. For low atomic number elements there exists a discrepancy of 10-20% between the experimental and theoretical values of L/K capture ratios. For Co^{58}, the recently reported

experimental value of L/K capture ratio is about 20% higher (Mollyer, 1961) than the theoretically predicted value of 0.092 used by Konijn et al (1958) and by Ramaswamy (1959) to determine K/β^+ ratio and the value of b.

In view of this, a direct determination of K-capture/β^+ ratio of Co^{58} was undertaken. The isotope Co^{58} possesses all the essential features for the assessment of b. As pointed out above, the decay is pure Gamow-Teller so that the result on b can be readily interpreted. Besides, the theoretical K-capture/β^+ ratio has been recently calculated by Nguyen-Khac (See Depommier et al, 1960) at 4.87 with 472 KeV for the positron end point energy. His calculation is based on the graphs of Brysk and Rose (1955,58) for the K electron radial wave functions and the tables of positron emission with second order correction by Dzelepov and Zirianova (1952). He has also taken into account the screening effect for positrons. The present direct measurement gives a result for the K-capture/β^+ ratio free from the uncertainties associated with the indirect method. The experimental accuracy

has been increased considerably and gives a more accurate value for b than obtained previously.

2. Source Preparation and Purity Check.

The Co^{58} was produced by the fast neutron reaction Ni^{58} (n,p) using a high pile factor at U.K.A.E.A., Harwell. The source was separated chemically at Amersham to free it from other radioactive impurities and was supplied as a carrier-free chloride. The Co^{60} content was specified as less than ½%. The specific activity was 100 μc/ml.

In order to establish the radiochemical purity of the sample, it was necessary to make a thorough radioactivity check. The gamma-radiations were checked by using an external Co^{58} source and a 2" x 2" NaI(Tl) crystal mounted on a E.M.I. 9514S photomultiplier. The source was mounted between two thin slabs of perspex. Aluminium sheet was used to absorb the β^+ radiations, and the source-detector distance kept at 4". The photomultiplier-crystal assembly was shielded with 2" of Pb provided with a 5 mm copper lining to absorb Pb x-rays. The pulses were amplified in a N.E. 5202

non-blocking amplifier and displayed in a C.D.C. multichannel pulse height analyser. Except for the two prominent peaks at 810 KeV and 510 KeV, no other radiations were observed in the region from 100 KeV to 2 MeV. Calibration was effected by external Hg^{203} (279 KeV), Na^{22} (510 KeV and 1.27 MeV), Cs^{137} (661 KeV) and Co^{60} (1.17 MeV and 1.33 MeV) gamma-ray standard sources. The gamma-spectrum from Co^{58} is shown in figure 29 . The background effects were small and have not been shown.

To confirm still further the absence of Co^{60} impurity a trace of Co^{58} was mounted in a plastic capsule. The wall of the capsule was about 2 mm thick and would completely absorb the beta particles. This was inserted in the central well $\frac{1}{4}$" diam x $1\frac{1}{4}$" deep of a 2" diam x 2" NaI(Tl) crystal. The Co^{60} decays in cascade with the emission of 1.17 and 1.33 MeV γ-rays and should therefore give a sum peak at 2.5 MeV region. No such peak was observed and it was estimated by comparison with the 810 KeV peak of Co^{58} that the Co^{60} content was less than $^{1}/_{10}\%$ of the total activity. The detection efficiency of the 810 KeV, 1.17 + 1.33 MeV

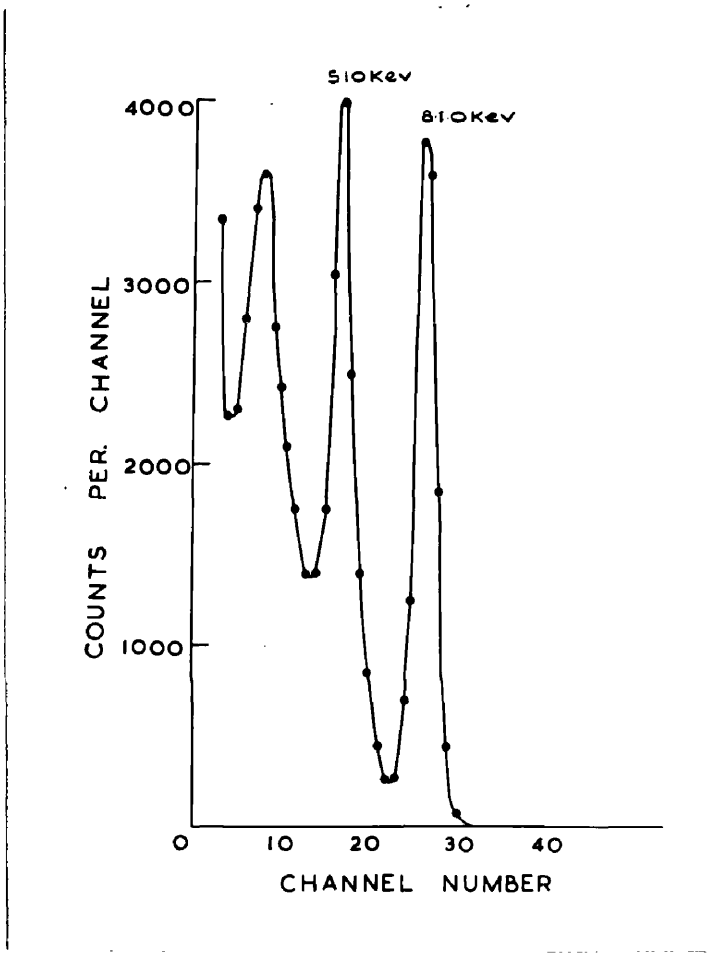

Fig. 29.

Co^{58} gamma-spectrum in a 2" crystal with an external source.

peaks in the crystal was taken into consideration in making this estimate. The low yield of Co^{60} is consistent with the thoretical prediction by Hughes (1954) and reported by Dagley et al (1958).

3. Experimental Procedure.

For the measurement of the K-capture and β^+ events a thallium activated sodium iodide crystal approximately 1 cm diam x $1\frac{1}{4}$ cm was grown with one drop of the Co^{58} source. The crystal when grown was washed with absolute alcohol, cut and polished to an area 4mm x 8 mm and thickness 2 mm. It was mounted in an aluminium container fitted with a thin glass window, with magnesium oxide as reflector. Optical contact between the glass window and the crystal surface was obtained by using silicone fluid. Excess of the silicone fluid from the sides of the crystal were removed before packing with Mgo. An E.M.I. 9514S phototube was used. Pulses were amplified in a non-blocking amplifier and displayed in a C.D.C. Kicksorter.

The K-capture events which consist of the K x-rays and K Auger electrons were completely absorbed in the

active crystal. Most of the β^+ particles will be wholly absorbed in the crystal. A few per cent of the high energy components of the β^+ particles, liberated near the surface of the crystal, could leave the crystal before losing all their energy. However, this would not affect the total β^+ counting rate. Preliminary experiments were carried out with the arrangement described above to check the performance of the system. A prominent peak was observed, figure 30, the energy of which was found to be about 7 KeV by comparison with the 46.5 KeV calibration peak. This corresponds to the K-absorption energy of iron. The gain was decreased and the β^+ spectrum was analysed as before. This spectrum is shown in figure 31. The two bumps at the higher energy channels are due to the distortion produced in the β^+ spectrum from the small compton distribution of the associated 510 and 810 KeV gamma-radiations in the active crystal.

To measure the K-capture/β^+ ratio a simple coincidence system was used. This is illustrated in figure 32. The pulses from the main counter were amplified in a non-overloading amplifier and fed by delay cable into a gating unit. This gate was controlled by the gamma-counter described below. Pulses from the activated

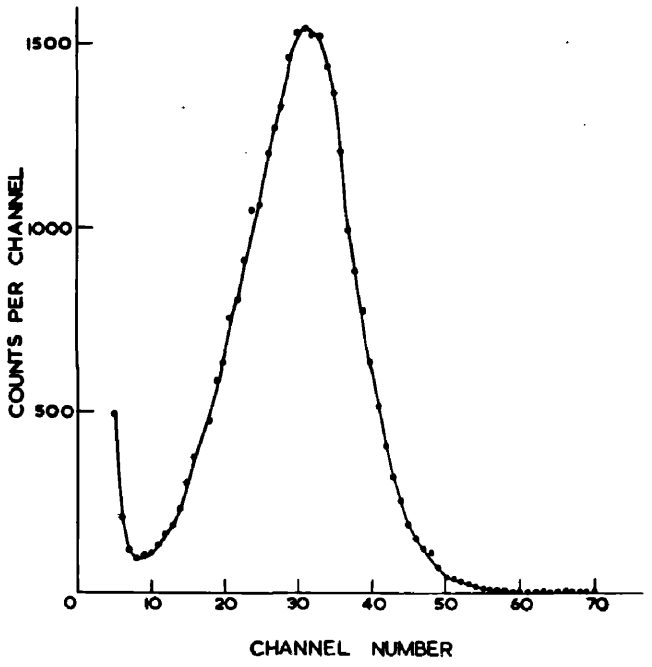

Fig. 30.

Co^{58} K-peak at about 7 KeV with an internal source (1 min. run).

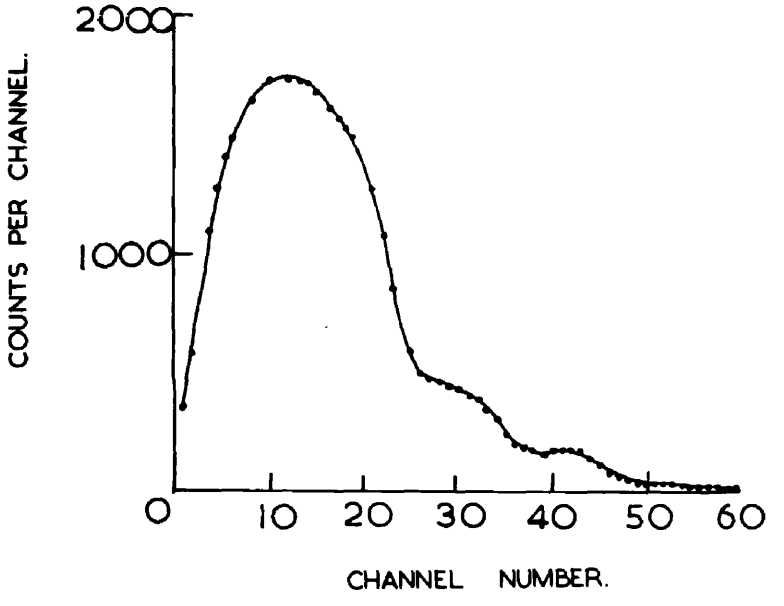

Fig. 31.

$Co^{58}\beta^{+}$ spectrum with an internal source (5 min. run).

crystal which were in coincidence with the peak of the 810 KeV radiation in the gamma-counter could be analysed in a multichannel pulse height analyser.

A 2" diam x 2" NaI(Tl) scintillator was mounted on another E.M.I. 9514S photomultiplier and this was used as a gamma-ray detector. The centre of this crystal was set at a distance of 4" from the small active crystal and was left undisturbed throughout the experiment. The detectors were shielded with 4" of lead to cut down room and cosmic-ray background. Pulses from the gamma-ray counter were amplified in a 1430A Dynatron pulse amplifier and were led to an I.D.L. single channel kicksorter. The "window" of the single channel kicksorter was set at the 810 KeV peak. This was effected by allowing the gamma-ray gating pulse to display its own spectrum. The position of this gamma-ray "window" setting is shown by the arrows in figure 33. The output from the I.D.L. single channel kicksorter was directed to a univibrator which generated a square pulse 5 μ sec wide and 30 volt high. This was used for gating K-capture and β^+ events from the small active crystal which were in coincidence with the 810

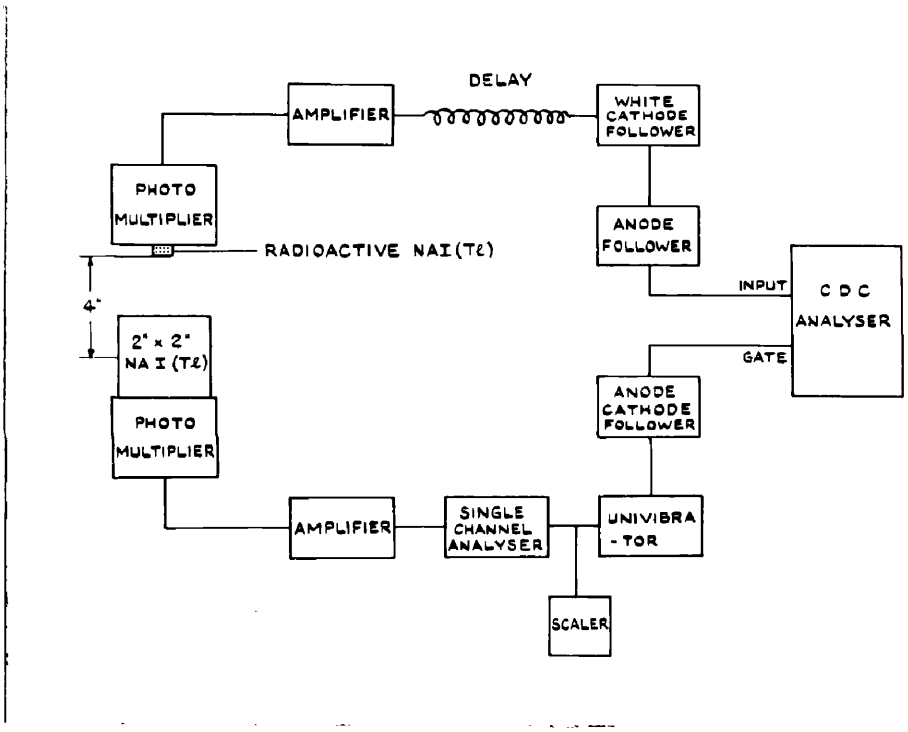

Fig. 32.

Block diagram of the coincidence system.

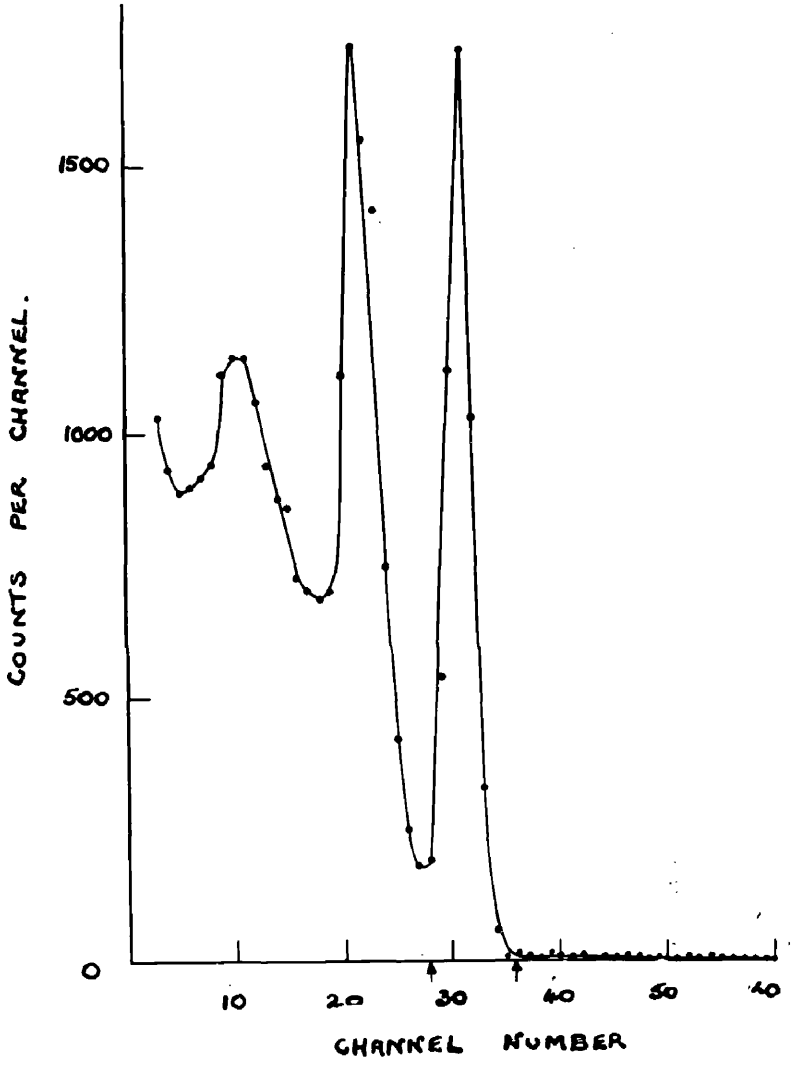

Fig. 33.

Co^{58} gamma-ray spectrum in a 2" crystal in coincidence with K-capture and β^+ events in the source crystal. The arrow shows the single channel kick-sorter "window" setting.

KeV peak. The main pulses were delayed by 2 μ sec with respect to the gating pulses to ensure complete overlap. The K-capture and β^+ events were analysed in separate runs by changing the gain of the amplifier. Before the start of the coincidence runs, the system had been left on to stabilise for more than 3 hours. Moreover, the stability was checked at frequent intervals by noting the counting rate at the single channel output and by allowing the gamma-ray gating pulse to display its own spectrum. No gain shifts were observed.

4. Results and Discussion.

Figure 34 and 35 show the typical K-capture and β^+ spectra obtained by taking coincidence with 810 KeV peak. The distortion produced at the higher energy side of the β^+ spectrum is due to the absorption of the associated 510 KeV annihilation radiation in the crystal. Several runs were taken of K and β^+ events in alternate order. The consistency of the runs is shown in table II. During the course of the experiment the active crystal was cleaned in alcohol and polished several times,

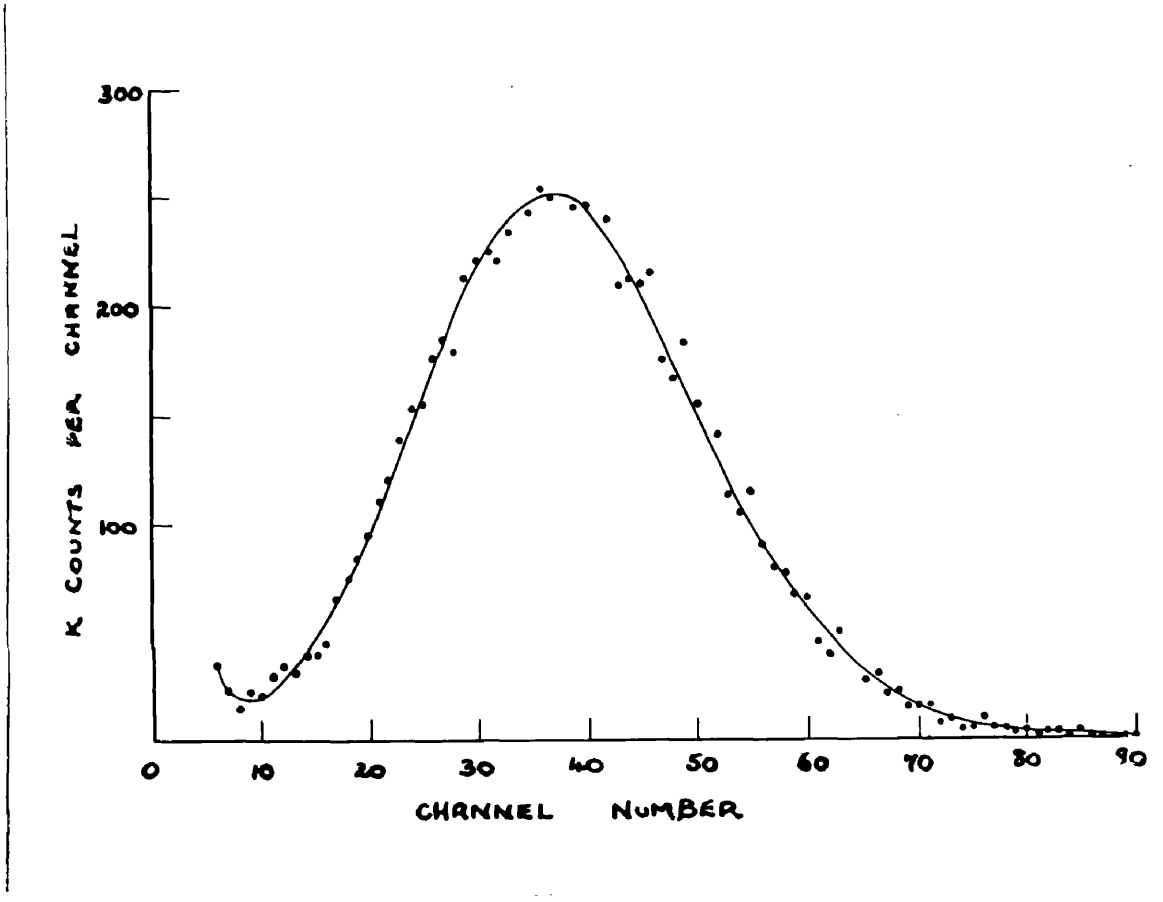

Fig. 34.

Co^{58} K-peak, with an internal source, in coincidence with 810 KeV gamma-ray peak (1 hr. run).

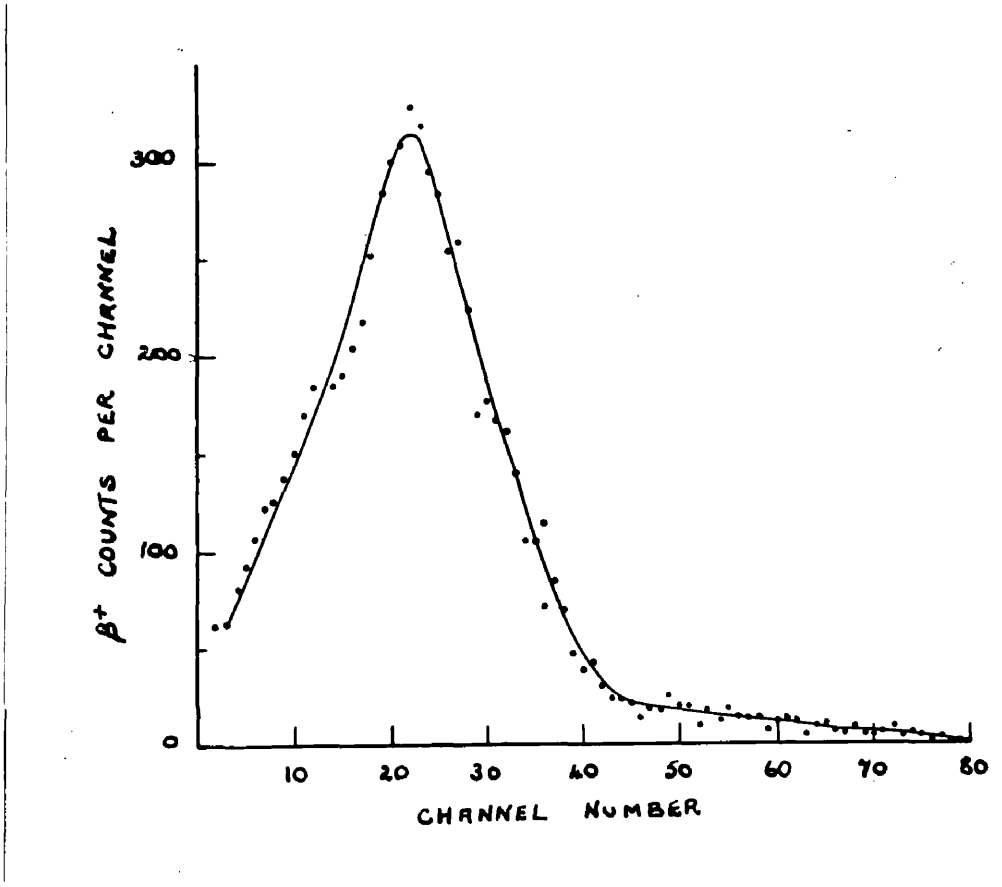

Fig. 35.

$Co^{58}\beta^+$ spectrum, with an internal source, in coincidence with 810 KeV gamma-ray peak ($4\frac{1}{2}$ hr. run).

Table II

Observed uncorrected K-capture/β^+ ratio.

Run	1	2	3	4	5	6	7	8
K/β^+ratio	4.94	4.97	4.95	4.91	4.91	4.93	4.93	4.96

The K-events were each generally having the order of 10,000-20,000 and β 5,000 counts.

changing its size by about a quarter. The consistency of the results showed that there were no surface effects due to source distribution.

In order to assess the chance coincidence rate an additional appropriate delay cable was inserted in the main channel. An examination in a fast oscilloscope indicated that the main pulse was well clear of the gating pulse. The gain of the amplifier was increased fractionally to adjust the pulse height losses due to the ohmic resistance in the extra delay line. The chance coincidence rate was 2% for both K-capture and β^+ events and did not affect the ratio observed. These random counts are not subtracted from the K-capture and β^+ spectra shown in figures 34 and 35 . The K-capture/β^+ branching ratio was obtained from the total number of counts in the K-peak and the β^+ spectrum.

The possibility of error that could arise in the main run due to the simultaneous detection of the 510 KeV annihilation and 810 KeV radiations in the gamma-counter was examined. This was necessary as it could affect the β^+ contribution. The gamma-spectra in coincidence with the K-capture and β^+ events were

analysed separately in the 2" counter. This was achieved by gating the gamma-spectrum with the K peak and the β^+ spectrum in the active crystal respectively. The geometry of the counter arrangement was not disturbed. The spectra so obtained are shown in figures 36 and 37 . The correction from this effect was found to be practically negligible ($^1/_{5}\%$).

Occasionally 810 KeV gamma-rays in coincidence with the K-capture events can produce a low energy (10-100 KeV) Compton electron in escaping from the active 2 mm thick crystal and still record in the 810 KeV gate. Such an event would be fallaciously registered as a β^+ event. To calculate this correction from the absorption coefficient data, the source was shown to be distributed symmetrically about the appropriate central face of the active crystal. This was done by using the active crystal as an external source and a 1 cm^2 x 2 mm thick NaI(Tl) crystal as a detector. The active crystal was kept in close proximity to the thin crystal and the relative intensity of the Compton distribution of the gamma-rays from either sides of the active crystal was measured. The choice of the thin crystal

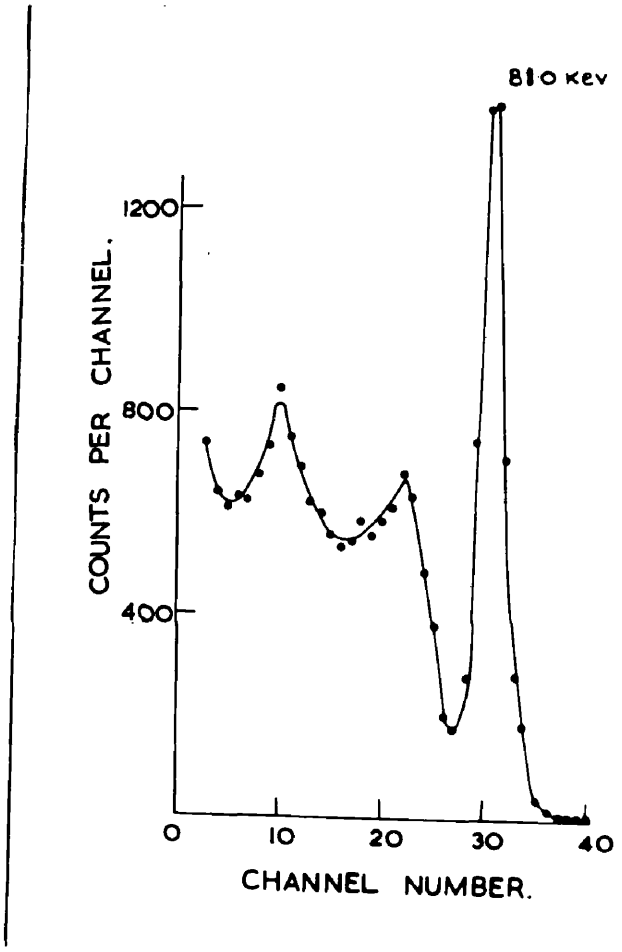

Fig. 36.

Co^{58} gamma-spectrum in the 2" crystal in coincidence with the K-peak in the source crystal.

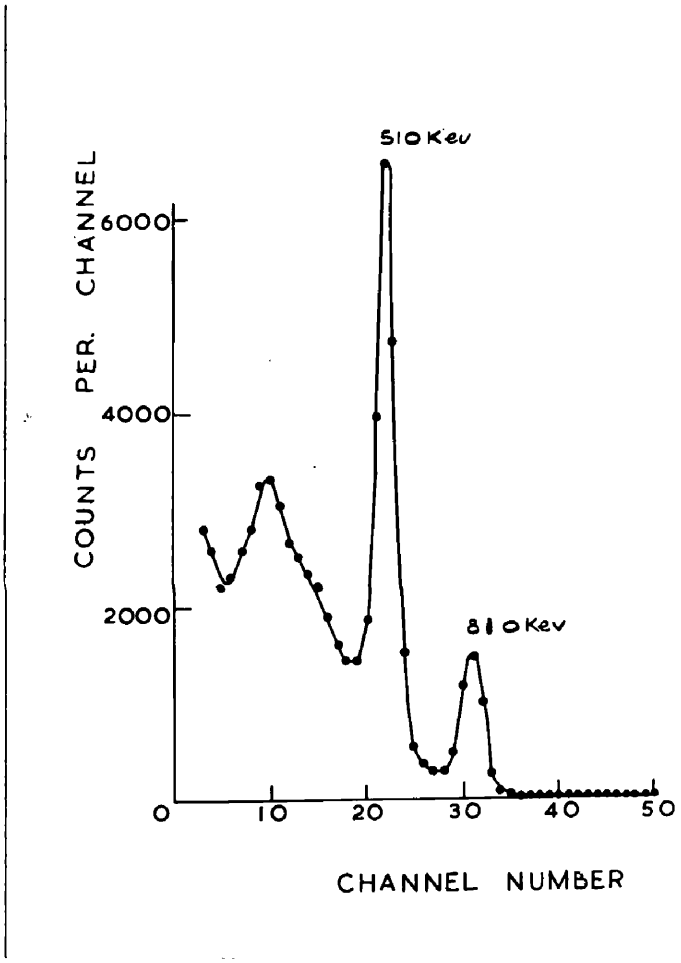

Fig. 37.

Co^{58} gamma-spectrum in the 2" crystal in coincidence with the β^+ spectrum in the source crystal.

was to minimise the error associated with the possible small change in solid angle when the active crystal was turned upside down.

It was necessary to make allowance for the weak K-capture branch emitted in the transition to the 1.62 MeV level, which would be in coincidence with the cascade 810 KeV and 810 KeV gamma-rays. In view of the large experimental uncertainty (of about 30%) in the data given in the decay scheme shown in figure 28 , a more precise value was required. This could be obtained more accurately here as in the present experiment it was possible to know any source strength by comparison with that of the active crystal whose K-capture counting rate was known. The inset in figure 38 shows the experimental arrangement for these measurements. The two counters were fitted each with 2" diam x 2" NaI(Tl) Harshaw scintillators and were oriented at 90^{o} so that the annihilation radiations which occur at 180^{o} do not interfere in the measurements. The lead block was $\frac{1}{2}$" thick and would prevent any quanta backscattered from one crystal from entering the other. The Co^{58} source was mounted in a plastic capsule holder and was placed

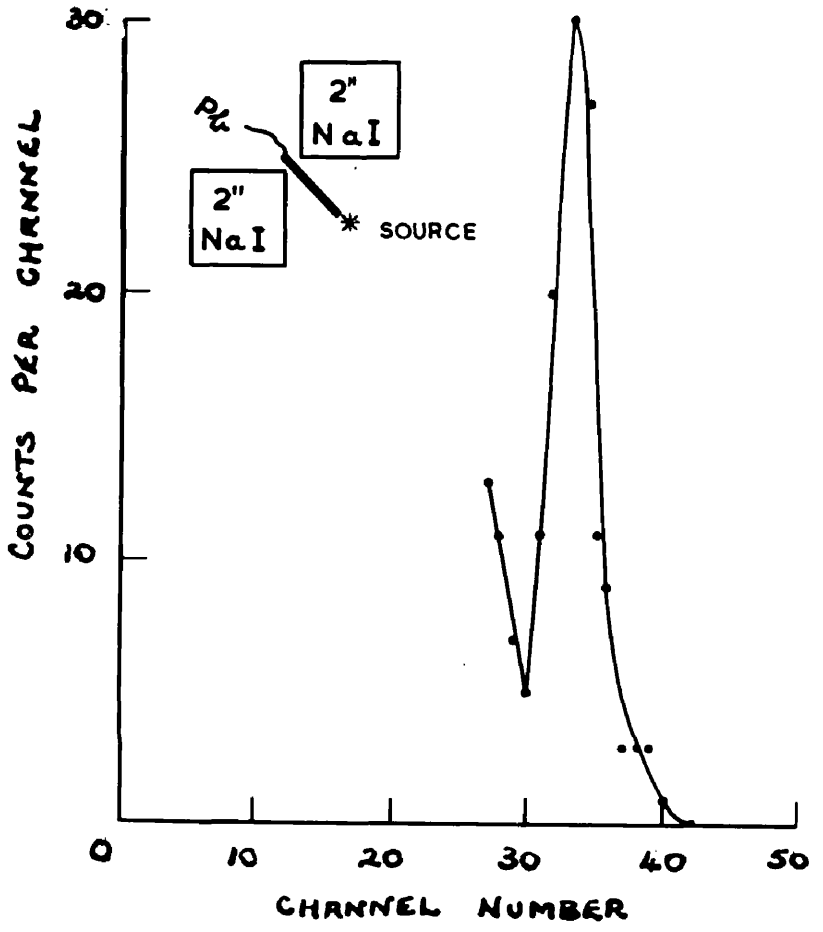

Fig. 38.

Investigation of the weak capture branch: Peak in the 800 KeV region obtained by gamma-gamma coincidence measurements. The inset shows the experimental set up.

at the intersection of the axes of the two crystals at a distance approximately $1\frac{3}{4}$" from their faces. The total amount of backscattering at the source was estimated to be negligibly small. On one side a single channel kicksorter with the "window" set at the 810 KeV peak was used and the other side employed a discriminator with the bias set at about 700 KeV. A coincidence unit with a resolving time of 1 μ sec was used. This operated a gate unit which generated a gating pulse of 10 μ sec and the associated spectrum from either side could be displayed on the multichannel kicksorter. Figure 38 shows the spectrum from the counter with the bias set at about 700 KeV. The random counting rate was found by inserting a delay of 4 μ sec between the single channel output and the coincidence unit. This was very small and was neglected. The fraction of the small K-capture branch to the 1.62 MeV state which subsequently proceeded to the 810 KeV level by gamma-emission was found to be (1.1 ± 0.1)% of the main K-capture branch. The experimental value of L/K capture ratio of 0.104 obtained by Moller (1951) was used to assess the K-capture contributions. The correction due

to this small effect was allowed for in the K-capture/β^+ ratio measurement.

Taking the mean of several measurements, the K-capture/β^+ ratio was found to be 4.92 ± 0.09. This data was corrected for the weak K-capture branch and the Compton escape, referred to above. The experimental error limit was partly due to statistics, but mainly due to the assessment of the low energy end of the K-peak. This being a coincidence measurement, there is no error at low energies from photomultiplier thermal noise and from the afterglow effects. The chance coincidence rate was low at all energies observed. The L-capture peak which would occur at 850 eV, in the region of single photoelectron emission, would be contributing partially at the trough of the K-peak. The low energy end of the K-peak was established by fitting a statistical distribution (W.B. Lewis 1942) to assess the scintillation counter efficiency. Further confirmation of the validity of the assessment of the K-peak was obtained from studies made recently with the active crystal using a new, more efficient E.M.I. 9514S photomultiplier. This K-capture peak, obtained without

coincidence, is shown in figure 8 .

The theoretical value of the K-capture/β^+ ratio for Co^{58} has been calculated by Nguyen-Khac (1960) with Brysk and Rose's curves for the radial functions of the bound electron and tables for β^+ emission by Dzelepov and Zerianova (1952) with second order corrections. Nguyen-Khac has also corrected the β^+ functions for screening effects given by Reitz (1950) and for nuclear radius calculated by Rose and Holmes (1951). The calculated value was Ro = 4.87 based on the assumption of the vanishing of the interference terms. Because of the uncertainty of 6 KeV in the published values of 472 KeV for the β^+ end point the theoretical value would become 4.87 ± 0.18. The value of $(\frac{1}{W})_{av}$ was calculated to be 0.75, by graphical integration of the theoretical β^+ spectrum.

To evaluate the Fierz Interference Term the theoretical and experimental (R) values of the K-capture/β^+ ratios and the value for $(\frac{1}{W})_{av}$ were inserted in equation (23) of Chapter I

$$b = \frac{R - R_o}{R_o + R(\frac{1}{W})_{av}}$$

here $R = \frac{K}{\beta^+}$, $R_o = (\frac{K}{\beta^+})_{b=o}$ and γ is neglected.

which gave b =+0.006 $\pm$ 0.023. The error limit is mainly associated with the uncertainty of the calculated K-capture/β^+ value, which is critically dependent on the β^+ end point energy. The 6 KeV uncertainty in the end point energy gives 4% variation in the theoretical value as compared to 2% in the experimental result. Previously this uncertainty has been neglected or underestimated.

The results obtained here can be unterpreted in either of two ways. The low experimental value of b accords within the error limits with the customary two-component neutrino theory, where $C_A = C_A'$, and $C_T = -C_T'$, and where b should vanish identically (equ.(20). Ch.I). In this form, the theory will require complete polarisation of β-particles at high energies (equ.(27). Ch.I). However, if the alternative possibility of the two component neutrino theory be adopted instead, where $C_A = C_A'$, and $C_T = + C_T'$, then $0 \leqslant \frac{C_T}{C_A} < 0.015$ follows directly from relation (20) (Ch.I). At the lower limit, of course, the two interpretations are identical.

Chapter VII.

Conclusion and Future Prospects.

Present Work.

The results on the simple allowed decay of Cs^{131} and the "unique" first forbidden decay of Tl^{204} are the first direct experimental measurements on the L/K capture ratios for the middle and high atomic number elements respectively. By virtue of the well-type internal source scintillation counter method the K and L capture X-rays or Auger electrons are completely detected and hence the results are free from the uncertainties regarding the assumptions of the K and L fluorescence yields and the knowledge of the K_α group. These experimental results confirm the validity of the relevant theory within the experimental errors. The work on Ba^{131} illustrates the general application of the technique for coincidence counting. The results obtained here are shown in figure 39. (compare figure 1).

The present work with internal source scintillation counter technique on the K-capture/β^+ branching ratio in the pure Gamow-Teller decay of Co^{58} shows the smallness of Fierz interference term . This is consistent with the customary two-component neutrino theory and the recent β-decay data. In this experiment the two main possible

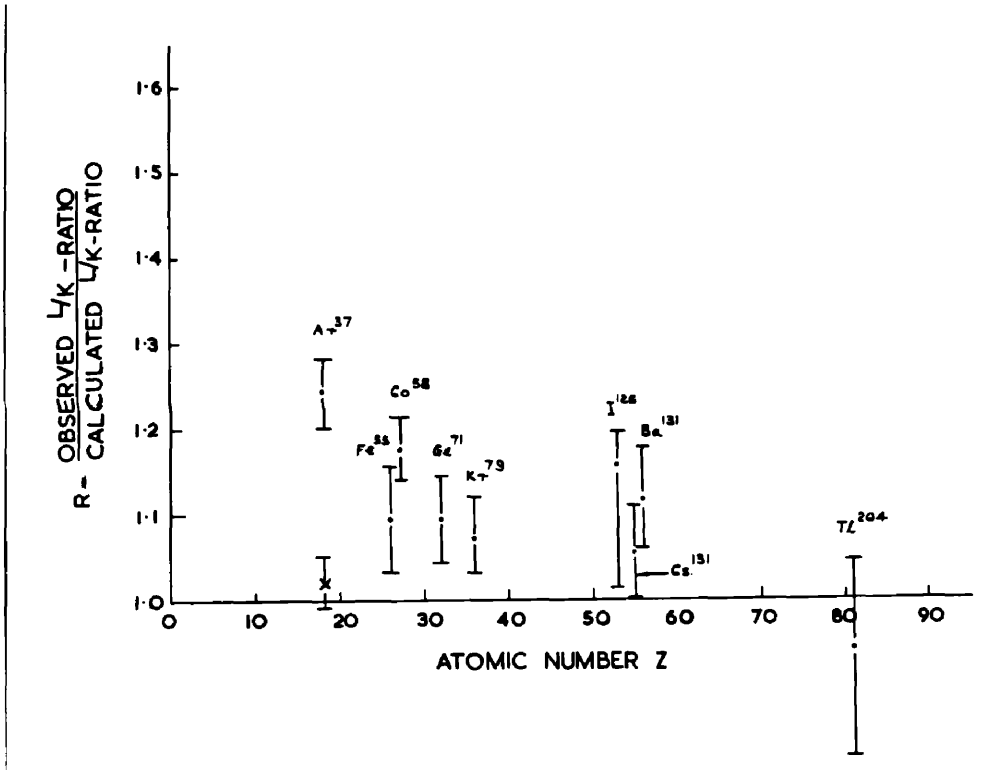

Fig. 39.

Comparison of the experimental and the calculated L/K capture ratios as in figure 1 together with the results obtained by the author on Cs^{131}, Ba^{131} and Tl^{204}.

sources of error, arising from the estimation of counter detection efficiency and the assumption of L and higher shell contributions, which may have been present in some of the earlier experiments with solid source techniques have been eliminated. It is considered, therefore, that the present value of b is the best for the Gamow-Teller decay.

Future Prospects.

Examination of figure 39 indicates that, at this stage, more experimental and theoretical works are necessary for low atomic number elements to resolve the 10-20% discrepancy between the experimental and calculated values. For middle and high atomic number elements, however, it would now be possible to use the observed L/K values for the determination of transition energies. Attention should, however, be restricted for allowed and "unique" decays. Moreover, accurate L/K ratio measurements for forbidden transitions could yield information regarding the magnitudes of nuclear matrix elements. For this application, it would be advisable to concentrate on those forbidden cases in which the transition energies are low enough so that the relative magnitudes of the matrix elements are significant.

The K-capture/β^+ branching ratio is very sensitive to the β^+ end point energy and so a precise measurement of the branching ratios would be useful to determine the end point energies. This application could be valuable in the analysis of nuclear energy levels and could be a better method than β-spectral studies. However, it is desirable to restrict such analysis to allowed and "unique" transitions. In addition, branching ratio measurements would be useful for the estimation of second order correction and screening effects in the positron wave functions.

One of the most important applications of the internal source scintillation counter technique would be for the studies of higher order processes of internal bremsstrahlung continuous photons and the electron excitation resulting in the "shake off" electron to the bound or continuum states following electron capture transitions. The theoretical calculations of internal bremsstrahlung phenomena are given by Morrison and Schiff (1950) and further extended by Glauber and Martin (1954, 1956 and 1958) and that of K-electron excitation effects by Primakoff and Porter (1953). The experiments on internal bremsstrahlung spectral distribution has been mostly done by using an external source scintillation

spectroscopy and the measurements have not been extended to cover the low energy portion.

A summary of the experimental results up to 1960 on electron excitation effects is given by Lark and Perlman (1960) in connection with their work on Cs^{131}.

With the radioactive source incorporated inside the crystal and the whole placed on a small well provided at the centre of a large appropriate crystal, a direct determination of the bremsstrahlung distribution can be made. The bremsstrahlung quanta always follow either K capture or L capture events in coincidence. So the bremsstrahlung spectrum will be displaced to the higher energy region and will be quite distinct from the single K and L peaks. The potential efficiency of the technique is very high, being limited only by the competition from the "shake off" electron distribution associated with the electron excitation effects and the statistical spread of the single K capture peak. Its sensitivity is limited by the cosmic and room background effects and the presence of the naturally occurring radioactive K^{40} in the NaI(Tl) scintillator. It is also desirable that the source should be obtainable with high specific activity and free from radioactive contamination to a very high degree.

The probability of production of "shake off" electron varies inversely as the square of atomic number and hence for very low Z elements, for example Be^7, this effect can be expected to be of the order of a few percent relative to the electron capture events. In addition, if the transition proceeds to the ground state with the emission of a γ-ray, the coincidence counting method can be adopted which helps to reduce the background effects. However, for general investigation of "shake off" electron energy spectrum it is advisable to explore the possibility of using some lighter scintillators of comparable efficiency to NaI(Tl) so that the majority of the internal bremsstrahlung photons escape from the detector. It may also be possible to detect the two escaping K X-rays and use the resultant coincidence pulse to gate the "shake off" electron event.

REFERENCES

Alvarez, L.W., 1937, Phys. Rev., 52, 134.

Bannerman, R.C., Lewis, G.M., and Curran, S.C., 1951, Phil. Mag., 40, 1097.

Bellamy, E.H., and Smith, K.F., 1953, Phil. Mag., 44, 33.

Bernstein, W., Bjerknes, C., and Steele, R., 1958, Liquid Scintillation Counting (London, Paris, New York: Pergamon Press), p.74.

Bethe, H.A., and Bacher, R.F., 1936, Rev. Mod. Phys., 8, 82.

Boehm, F., Novey, T.B., Barnes, C.A., and Stech, B., 1957, Phys. Rev., 108, 1479.

Bouchez, R., and Depommier, P., 1960, Rep. Prog. Phys., 23, 395.

Bridgman, P.W., 1925, Proc. Amer. Acad. Arts Sci., 60, 350.

Brysk, H., and Rose, M.E., 1958, Rev. Mod. Phys., 30, 1169; Ibid., 1955, Oak Ridge National Laboratory Report, ORNL 1830.

Burhop, E.H.S., 1952, The Auger Effect (Cambridge: University Press).

Cheng, L.S., Dick, J.L., and Kurbatov, J.D., 1952, Phys. Rev., 88, 887.

Cook, C.S., and Tomnovec, F.M., 1956, Phys. Rev., 104, 1407.

Cork, J.M., Brice, M.K., and Schmid, L.C., 1955, Phys. Rev., 99, 703.

Dagley, P., Grace, M.A., Hill, J.S., and Sowter, C.V., 1958, Phil. Mag., 3, 489.

Daniel, H., 1958, Z. Physik, 150, 144.

Deniels, J.M., Grace, M.A., Halban, H., Kurti, N., and Robinson, F.N.A., 1952, Phil. Mag., 45, 1297.

Depommier, P., Nguyen-Khac, U., and Bouchez, R., 1960, Jour. de. Phys. et le Rad., 5, 456.

Der Mateosian, E., 1953, Phys. Rev., 92, 938.

Der Mateosian, E., and Smith, A., 1952, Phys. Rev., 88, 1186.

Deutsch, M., and Elliott, L.G., 1944, Phys. Rev., 65, 211.

Deutsch, M., Gittelman, B., Bauer, R.W., Grodzins, L., and Sunyar, A.W., 1957, Phys. Rev., 107, 1733.

Dobrov, W., and Jeffries, C.D., 1957, Phys. Rev., 108, 60.

Drever, R.W.P., and Moljk, A., 1957, Phil. Mag., 2, 427; See Robinson and Fink, 1960, for more recent values on Ge^{71} and Kr^{79}.

Drever, R.W.P., Moljk, A., and Curran, S.C., 1957, Nucl. Inst., 1, 41.

Drever, R.W.P., Moljk, A., and Scobie, J., 1956, Phil. Mag., 1, 942.

Dzelepov, B.S., and Zirianova, L.N., 1952, Tables pour la desintegration β Ed. de l'Universite de Leningrad.

Feister, I., 1952, Tables for the analysis of β Spectra (Washington: N.B.S. Applied Mathematics series No. 13).

Fermi, E., 1934, Z. Physik, 88, 161.

Fierz, M., 1937, Z. Physik, 104, 533.

*Fink, R.W., and Robinson, B.L., 1959, Nuclear Phys. 10, 82.

Finkle, B., 1947, Phys. Rev., 72, 1260.

Frauenfelder, H., Bobone, E., von Goeler, E., Levine, N., Lewis, H.R., Peacock, R.N., Rossi, A., and de Pasquati, G., 1957, Phys. Rev., 106, 386.

Frauenfelder, H., Levine, N., Rossi, A., and Singer, S., 1956, Phys. Rev., 103, 352.

Glauber, R.G., and Martin, P.C., 1954, Phys. Rev., 95, 572; 1956, Phys. Rev., 104, 158; 1958, Phys. Rev., 109, 1307.

*Fink, R.W., 1955, Phys. Rev. 98, 1293.

Goldhaber, M., and Hill, R.D., 1952, Revs. Mod. Phys. 24, 179.

Goldhaber, M. Grodzins, L., and Sunyar, A.W., 1958, Phys. Rev., 109, 1015.

Good, W.M., Peaslee, D., and Deutsch, M., 1946, Phys. Rev., 69, 313.

Grace, M.A., Jones, G.A., and Newton, J.O., 1956, Phil. Mag., 1, 363.

Grard, F., 1958, Physika., 24, 868.

Griffing, D.F., Wheatley, J.C., 1956, Phys. Rev., 104, 389.

Harrison, F.B., 1954, Nucleonics, 12, 24.

Harrmannsfeldt, W.B., Burman, R.L., Stahelin, P., Allen, J.S., and Braid, T.H., 1958, Phys. Rev. Letters, 1, 61; a confirmation of the He^6 result was reported by Pleasonton, F., Johnson, C.H., and Snell, A.H., Bull. Am. Phys. Soc., 1959, 4, 78.

Herrmannsfeldt, W.B., Maxon, D.R., Stahelin, P., and Allen J.S., 1957, Phys. Rev., 107, 641.

Hoppes, D.D., Hayward, R.W., 1956, Phys. Rev., 104, 368.

Hughes, D.J., 1954, Nature, London, 173, 396.

Jackson, J.D., 1958, The Physics of Elementary Particles (Oxford: University Press), p.100 and 116.

Jung, R.G., and Pool, M.L., 1956, Bull. Am. Phys. Soc. 1, No. 4, 172, E11.

Katcoff, S., 1947, Phys. Rev., 72, 1160.

Konijn, J., Van Nooijen, B., Hagedoorn, H.L., and Wapstra, A.H., 1958, Nuclear Phys., 9, 296.

Konopinski, E.J., 1957, Proc. Rehovoth. Conf. (Amsterdam: North-Holland).

Ibid., 1959, Annual Rev. of Nucl. Sci. 9, 99.

Landau, L., 1957, Nuclear Phys. 3, 127.

Langer, L.M., Price, H.C., 1949, Phys. Rev., 75, 1109.

Langevin, M., 1954, C.R., Acad. Sci., Paris, 238, 1518; 1955, J. Phys. Radium, 16, 516.

Ibid., 1956, Ann. Phys., 1, 57.

Lark, N.L., Perlman, M.L., 1960, Phys. Rev., 120, 536.

Lee, T.D., and Yang, C.N., 1956, Phys. Rev., 104, 254.

Ibid., 1957, Phys. Rev., 105, 1671.

Lewis, W.B., 1942, Electrical Counting (Cambridge: University Press), p.116.

Lidofsky, L., Maklin, P., and Wu, C.S., 1952, Phys. Rev. 87, 391.

Marshak, R.E., 1942, Phys. Rev., 61, 431.

Michalowicz, A., 1957, Ann. Phys., 2, 116.

Moler, R.B., 1961, Interim Progess Report NSF-G5050, App. IV, University of Arkansas.

Møller, C., 1937, Phys. Rev., 51, 84.

Morrison, P., and Schiff, L., 1940, Phys. Rev., 58, 24.

Nguyen-Khac, U., 1960 (See Depommier et al.)

Nuclear Data Sheets., 1958, National Academy of Sciences - National Research Council, 2101 Constitution Ave. Washington 25, D.C., U.S.A.

Odiot, S., Daudel, R., 1956, J. Phys. Rad., 17, 60.

Pauli, W., 1933, Handbuch d. Phys., 24, 1225.(Berlin: Springer).

Perlman, M.L., Welker, J.P., and Wofsberg, M., 1958, Phys. Rev., 110, 381.

Pontecorvo, B., Kirkwood, D.H.W., and Hanna, G.C., 1949, Phys. Rev., 75, 982.

Primakoff, H., and Porter, F.T., 1953, Phys. Rev., 89, 930.

Radvanyi, P., 1955, J. Phys. Rad., 16, 509.

Ramaswamy, M.K., 1959, Ind. Journ. Phys., 33, 285.

Reitz, J., 1950, Phys. Rev., 77, 10.

Robinson, B.L., and Fink, R.W., 1960, Rev. Mod. Phys., 32, 117.

Rose, M.E., and Holmes, D.K., 1951, Phys. Rev., 83, 190.

Rose, M.E., and Jackson, J.L., 1949, Phys. Rev., 76, 1540.

Salam, A., 1957, Nuovo Cimento, 5, 299.

Santos-Ocampo, A.G., and Conway, D.C., 1960, Phys. Rev., 120, 2196.

Saraf, B., 1954, Phys. Rev., 94, 642.

Scharff-Goldhaber, G., der Mateosian, E., Johnson, G.W., and McKeown, M., 1951, Phys. Rev., 83, 480.

Schuman, R.P., Jones, M.E., and Mewherter, A.C., 1956, J. Inorg. Nucl. Chem., 3, 160.

Scobie, J., and Gabathuler, E., 1958, Proc. Phys. Soc., 72, 437.

Scobie, J., and Lewis, G.M., 1957, Phil. Mag., 2, 1089.

Scobie, J., Moler, R.B., and Fink, R.W., 1959, Phys. Rev., 116, 657.

Sherr, R., and Gerhart, J.B., 1956, Bull. Am. Phys. Soc., 1, 219.

Sherr, R., and Miller, R.H., 1954, Phys. Rev., 93, 1076.

Siegbahn, M., (Ed), 1955, Beta and Gamma-Ray Spectroscopy (Amsteradm: North Holland Publishing Company).

Strauch, K., 1950, Phys. Rev., 79, 487.

Tayler, C.J., Jentschke, W.K., Remley, M.E., Eby, F.S., and Kruger, P.G., 1951, Phys. Rev., 84, 1034.

Vartapetian, H., 1956, Compt, Rend., 243, 1512.

West, H.I., Mayerhof, W.E., and Hofstadter, R., 1951, Phys. Rev., 81, 141.

Wright, H.W., Wyatt, E.I., Reynolds, S.A., Lyon, W.S., and Handley, T.H., 1957, Nuclear Sci. Eng., 2, 427.

Wu, C.S., Ambler, E., Hayward, R.W., Hoppes, D.D., and Hudson, R.P., 1957, Phys. Rev., 105, 1413. and 1957, Phys. Rev., 106, 1361.

Yaffe, L., Kirsch, M., Standil, S., and Grunlung, J.M., 1949, Phys. Rev., 75, 699.

Yu, F.C., Gideon, D., and Kurbatov, J.D., 1947, Phys. Rev., 71, 382.

Yakawa, H., and Sakata, S., 1935, Proc. Phys. Math. Soc. (Japan), 17, 467.

Zwiefel, P.F., 1954, Phys. Rev., 96, 1572, Ibid., 107, 329; 1958, Proceedings of the Rehovoth Conference on Nuclear Structure (Amsterdam: North-Holland).